

LUNDS TEKNISKA HÖGSKOLA

Design of Experiment Based on Full Factorial CFD Spray Modelling

Olle Faritzson

*Thesis for degree in Master of Science in Engineering, Mechanical
Engineering*



**LUNDS
UNIVERSITET**
Lunds Tekniska Högskola

DEPARTMENT OF ENERGY SCIENCES
DIVISION OF FLUID MECHANICS
FACULTY OF ENGINEERING, LUND UNIVERSITY
LUND, SWEDEN
JUNE 15, 2023

Abstract

Design of experiment is a powerful tool that can reduce the amount of physical testing needed to save resources, time and money. A CFD-setup was constructed in OpenFOAM-8, simulating injection of liquid propane with a standard multi-hole injector. The model was then validated against experimental results. Two design of experiment models were then created using Rstudio. The two models had four specified input parameters that were present in the CFD-model. The value of each parameter was then changed according to the respective DoE model and simulated. The two models were then evaluated and compared to each other. This was done by looking at two response variables and conducting ANOVA tests. Results showed some correlation between the two models. However significance factors and interactions differed to some degree between the two. A large effort was also put into comparing the models and evaluating tools for this purpose. This thesis lays a ground for future work developing a larger CFD-model, having a larger amount of changeable parameters. Furthermore it lays a ground for developing and optimising a DoE model as well as focusing on more tools for evaluating the acquired responses.

Acknowledgements

After 20 weeks of hard and interesting work at the Division of Fluid Mechanics, Faculty of Engineering at Lund University, in close collaboration with MAN Energy Solutions, I would like to thank my main supervisor Hesameddin Fatehi for all discussions, help and feedback during the whole process. I would also like to send gratitude to my supervisors at MAN Energy Solutions, Eric Baudoin and Simon Braamunch Ringsted, for all discussions and help regarding both OpenFOAM and Design of Experiments.

I would also like to send out gratitude to my family for always believing in me and supporting my decisions in life. Finally I would like to thank Sofia for supporting me and cheering me on throughout the whole process.

Contents

1	Introduction	3
1.1	Project motivation and Background	3
1.2	Project aims	3
2	Theory	5
2.1	Computational Fluid Dynamics	5
2.1.1	OpenFOAM	5
2.1.2	Governing Equations	5
2.1.3	Lagrangian Particle Tracking	7
2.1.4	K-epsilon Turbulence Model	8
2.1.5	Liquid Breakup and Breakup Models	8
2.1.6	Rosin-Rammler Particle Size Distribution	10
2.2	Liquefied Petroleum Gas	11
2.2.1	Flash Boiling	11
2.3	Design of Experiment	12
2.3.1	2^k Factorial Designs	12
2.3.2	Space Filling Designs	15
2.3.3	Analysis Of Variance Tests	16
3	Method	17
3.1	Method Overview	17
3.2	CFD-Case Setup	17
3.2.1	Geometry	17
3.2.2	Spray G Injection Profile	19
3.2.3	Boundary And Initial Conditions	20
3.2.4	Mesh	21
3.2.5	Mesh Sensitivity Analysis	23
3.2.6	Model Parameter Analysis	24
3.3	Design Of Experiment Setup	27
3.3.1	2^4 Factorial Design	27
3.3.2	Latin Hypercube Design	28
4	Results	30
4.1	CFD Results	30
4.2	Results - Design Of Experiment	34
4.2.1	2^4 Factorial Design	34
4.2.2	Latin Hypercube Design	38
5	Discussion	42
5.1	CFD Section	42
5.2	Design Of Experiment Section	42

6	Conclusions	44
6.1	Conclusions	44
6.2	Suggestion for future work	45
A	Plots Gaussian Process Modelling	48
A.1	Liquid Penetration	48
A.2	Vapor Penetration	49
B	R code	50
B.1	Contour Plots Lattice Hypercube Design	50
B.2	ANOVA Script	51
B.3	Latin Hypercube Design	52
B.4	2 ⁴ Factorial Design And Analysis	52

Chapter 1

Introduction

1.1 Project motivation and Background

The need for transportation services is growing in an ever globalizing world. At the same time, limiting global warming is one of the biggest challenges we stand in front of today. Standing for almost 3 percent of global greenhouse gas emissions, the maritime shipping industry is an important sector where greenhouse gas emissions need to be reduced [1]. To reach the Paris Agreement 1.5 C° trajectory, at least 5 percent of all shipping fuels needs to be climate-neutral by 2030 [1]. With the help of research and development we can find new climate-neutral ways of fueling the maritime shipping industry.

An important tool for research and development is experiments and experimental data. With the help of experiments and experimental data, it is possible to obtain a greater understanding of how and why a system acts the way it does. Using Design of Experiments (DoE) we can further accelerate the experimental procedure, giving us a greater understanding of how the system works and acts in different circumstances. With the help of experiments and DoE we can shorten the time to the ever so important move to sustainable and climate-neutral maritime transport.

Design of experiment is a branch of applied statistics that deals with planning, conducting, analysing and interpreting of controlled test to evaluate the value of one or a group of parameters. This is a very powerful tool and can be used in many experimental situations [2]. Using DoE one can mitigate the need for large in depth experiments and only change a handful of parameters to achieve the same desired effect or effects. A well planned DoE can give the research a meaningful data-set to act upon with the optimal number of experiments. This preserves resources that can be used for other important applications.

Computational fluid dynamics, (CFD), uses numerical analysis to examine and solve problems involving fluid flows. Using this, it is possible to solve and test complex fluid flows such as fuel spray injection in maritime engines. With the help of CFD a large number of parameters can be changed with ease to find differences between set-ups. With this tool one can reduce need of physical experiments, saving both money and time.

1.2 Project aims

The project will focus on Design of Experiments applied to computational experiments (3D-CFD). Furthermore, effort will be put into computer tool evaluation with highest priority on the programming languages R and Python.

The objective for the project is to find the optimal DoE approach to build an accurate response model in size and complexity. As a reference, a CFD-model representing direct fuel injection into a combustion chamber will be created and evaluated. The injection model will be created and simulated using OpenFOAM-8. The CFD-case will in first hand have Liquefied Petroleum Gas, LPG, injected into the chamber with the fall back

on Diesel. The model will then be analysed and compared to experimental data to ensure accuracy. After completion of the CFD-model, different experiment design methods should be analysed and compared. The models will be evaluated and used together with the CFD-model. The final DoE model should be:

- Complex enough for statistical analysis
- Simple enough so it can be fast and easy to deploy on a large scale
- It should allow one to define relevant target parameters (multi-objectives)
- It should allow one to define multiple design parameters
- Some experimental data should be available for validation

Chapter 2

Theory

2.1 Computational Fluid Dynamics

Computational fluid dynamics, CFD, is a branch within the field of fluid dynamics which utilizes numerical methods for predicting fluid flows and heat transfer in a number of applications.

2.1.1 OpenFOAM

The OpenFOAM CFD toolbox is a free, open source CFD software where OpenFOAM stands for Open Field Operation and Manipulation. The software has a large user base across several areas of engineering and science, both in academia and in the industry sector. OpenFOAM have a large range of features to solve problems ranging from complex fluid flows involving chemical reactions, turbulence, heat transfer to acoustics, solid mechanics and electromagnetics. For this thesis the sprayFoam solver will be used to model and simulate the spray injection and track the injected particles [3].

2.1.2 Governing Equations

Reynolds Averaged Navier-Stokes, (RANS), turbulence modelling is applied to the gaseous phase, thus the phase is described with the averaged Navier-Stokes partial differential equations. As the flow cannot be assumed to be incompressible, it is described with the Favre averaged Navier-Stokes equations. This means that the equations are density and time averaged, the procedure is shown below [4].

Time averaging for any dependent variable, Φ :

$$\bar{\Phi} = \frac{1}{T} \int_T \Phi(t) dt \quad (2.1)$$

$$\Phi = \bar{\Phi} + \Phi' \quad (2.2)$$

Density weighted time averaging of Φ :

$$\tilde{\Phi} = \frac{\overline{\rho\Phi}}{\bar{\rho}} \quad (2.3)$$

$$\Phi = \tilde{\Phi} + \Phi'' \quad (2.4)$$

The Favre-averaged Navier-Stokes equations are given in equations 2.5, 2.6, 2.8 and 2.9 below [5]:

Continuity

$$\frac{\partial \bar{\rho}}{\partial t} + \frac{\partial}{\partial x_j} (\bar{\rho} \tilde{u}_j) = \overline{S_\rho}^s \quad (2.5)$$

Momentum

$$\frac{\partial}{\partial t}(\bar{\rho}\tilde{u}_i) + \frac{\partial}{\partial x_j}(\bar{\rho}\tilde{u}_i\tilde{u}_j) = -\frac{\partial}{\partial x_j} \left(-\bar{p}\delta_{ij} + \bar{\tau}_{ji} - \overline{\rho u_i'' u_j''} \right) + \overline{S_{u,i}}^s \quad (2.6)$$

where $-\overline{\rho u_i'' u_j''}$ is the Reynolds-stress tensor and τ_{ij} is the viscous stress tensor defined as:

$$\tau_{ij} = \mu \left(\frac{\partial u_i}{\partial x_j} + \frac{\partial u_j}{\partial x_i} - \frac{2}{3} \frac{\partial u_k}{\partial x_k} \delta_{ji} \right) \quad (2.7)$$

Species transport

$$\frac{\partial}{\partial t}(\bar{\rho}\tilde{Y}_i) + \frac{\partial}{\partial x_j}(\bar{\rho}\tilde{Y}_i\tilde{u}_j) = \frac{\partial}{\partial x_j} \left(\bar{\rho}D \frac{\partial \tilde{Y}_i}{\partial x_j} - \overline{\rho u_j'' Y_i''} \right) + \overline{S_{\rho,i}}^s \quad (2.8)$$

where D is the mass diffusion coefficient and $\overline{\rho u_j'' Y_i''}$ is the Reynolds species flux vector.

Energy

$$\frac{\partial}{\partial t}(\bar{\rho}\tilde{E}) + \frac{\partial}{\partial x_j}(\bar{\rho}\tilde{u}_j\tilde{E}) = \frac{\partial}{\partial x_j} (-\bar{p}u_j + \bar{u}_i\bar{\tau}_{ji} - \bar{q}_j - \overline{\rho u_j'' E''}) + \overline{S_E}^s \quad (2.9)$$

where $\overline{\rho u_j'' E''}$ is the Reynolds energy flux vector and \tilde{E} is the total energy defined as:

$$\tilde{E} = \tilde{e} + \frac{\tilde{u}_i\tilde{u}_i}{2} \quad (2.10)$$

and q_j is the heat flux vector defined as:

$$q_j = -\lambda \frac{\partial T}{\partial x_j} \quad (2.11)$$

where λ is the thermal conductivity, T the temperature and e the internal energy.

The terms $\overline{S_\rho}^s$, $\overline{S_{\rho,i}}^s$, $\overline{S_{u,i}}^s$ and $\overline{S_E}^s$ are source terms introduced due to the two-way coupling which takes the evaporation of the discrete phase into account. S_ρ is the gaseous sphere evaporation rate of all spray parcels in the cell given by:

$$S_\rho = -\frac{1}{V_{cell}} \sum N_p \frac{dm_{gs}}{dt} \quad (2.12)$$

where m_{gs} is the mass of a single gaseous phase sphere and N_p is the number of spheres in the parcel. The time derivative of m_{gs} is the evaporation rate of a gaseous sphere and is given by the expression below:

$$\frac{dm_{gs}}{dt} = \dot{m}_{gs} = -\frac{m_{gs}}{\tau_e} \quad (2.13)$$

where τ_e is an evaporation relaxation time.

Similarly to S_ρ , the rate of momentum change, $S_{u,i}^s$ can be expressed as:

$$S_{u,i}^s = -\frac{1}{V_{cell}} \sum N_p m_{gs} \frac{du_{gs,i}}{dt} \quad (2.14)$$

where the acceleration of the gaseous sphere $\frac{du_{gs,i}}{dt}$, can be written as:

$$\frac{du_{gs,i}}{dt} = -\frac{u_{gs,i} - u_i}{\tau_{u,i}} = -\frac{u_{rel,i}}{\tau_{u,i}} \quad (2.15)$$

Here $\tau_{u,i}$ is a momentum relaxation time that is a function of droplet size, velocity, density and drag coefficient. This means that the only forces that act on the gaseous particles is the drag force. The drag coefficient, C_D can be calculated as [6]:

$$C_D = \begin{cases} \frac{24}{Re_{gs}} (1 + \frac{1}{6} Re_{gs}^{2/3}) & Re_{gs} \leq 1000 \\ 0.426 & Re_{gs} > 1000 \end{cases} \quad (2.16)$$

Re_{gs} is the Reynolds number for a gaseous sphere:

$$Re_{gs} = \frac{\rho|u_{rel,i}|d_{gs}}{\mu} \quad (2.17)$$

As above for S_ρ^s , $S_{\rho,i}^s$ can be expressed as:

$$S_{\rho,i}^s = -\frac{1}{V_{cell}} \sum N_p \frac{dm_{gs,i}}{dt} \quad (2.18)$$

S_E^s is the source term that accounts for exchange of energy between the phases and it can be expressed as:

$$S_E^s = -\frac{1}{V_{cell}} \sum N_p m_{gs} \frac{dh_{gs}}{dt} \quad (2.19)$$

The droplet temperature change is given by:

$$\frac{dT_{gs}}{dt} = \frac{T - T_{gs}}{\tau_h} f - \frac{1}{c_{l,gs}} \frac{h_v T_{gs}}{\tau_e} \quad (2.20)$$

where $c_{l,gs}$ is the liquid specific heat and τ_h is a characteristic heat transfer relaxation time [5].

2.1.3 Lagrangian Particle Tracking

To track the spray particle phase and solve its interaction with the continuous phase during the injection the Lagrangian particle tracking, (LPT), method is used. The method uses the Lagrangian approach where each property of the particles is a function of the position (x, y, z) of the particle and the time t . If the value of a property per unit mass is denoted by ϕ , the total or substantive derivative of ϕ with respect to time is:

$$\frac{D\phi}{Dt} = \frac{\partial\phi}{\partial t} + \frac{\partial\phi}{\partial x} \frac{dx}{dt} + \frac{\partial\phi}{\partial y} \frac{dy}{dt} + \frac{\partial\phi}{\partial z} \frac{dz}{dt} \quad (2.21)$$

The fluid particle will follow the flow so, $dx/dt = u$, $dy/dt = v$ and $dz/dt = w$. Thus the substantive derivative of ϕ is given by:

$$\frac{D\phi}{Dt} = \frac{\partial\phi}{\partial t} + u \frac{\partial\phi}{\partial x} + v \frac{\partial\phi}{\partial y} + w \frac{\partial\phi}{\partial z} = \frac{\partial\phi}{\partial t} + \mathbf{u} \cdot \text{grad}\phi \quad (2.22)$$

$D\phi/Dt$ defines rate of change of property ϕ per unit mass [7].

The individual particles are tracked from injection until an integration limit criterion is achieved or if they leave the domain. The particles are injected in turn to obtain an average of all the particle tracks and to generate source terms to the fluid mass, momentum and energy equations [8].

To calculate the particle trajectory and velocity, the relevant forces acting on the particles needs to be taken into consideration. If spherical particles are considered, the differential equations for calculating the particle location and velocity is given by Newtonian second law:

$$\frac{dx_P}{dt} = u_P \quad (2.23)$$

$$m_P \frac{du_P}{dt} = \sum F_i \quad (2.24)$$

$$I_P \frac{d\omega_P}{dt} = T \quad (2.25)$$

where $m_P = \rho_P d_P^3 \pi / 6$ is a particle mass, $I_P = 0.1 m_P d_P^2$ is the moment of inertia, F_i represents the relevant forces acting on the particle, ω_P is the angular velocity of the particle and T is the torque acting on a rotating particle due to the viscous interactions with the fluid [9].

2.1.4 K-epsilon Turbulence Model

To model the turbulence, the k- ϵ turbulence model is used. This model is a two equation model where the transport equations are solved for the two turbulence quantities k and ϵ [10]. The k- ϵ model consists of the model transport equation for k:

$$\frac{\partial(\rho k)}{\partial t} + \frac{\partial(\rho k u_i)}{\partial x_i} = \frac{\partial}{\partial x_j} \left[\frac{\mu_t}{\sigma_k} \frac{\partial k}{\partial x_j} \right] + 2\mu_t E_{ij} E_{ij} - \rho \epsilon \quad (2.26)$$

the model transport equation for ϵ :

$$\frac{\partial(\rho \epsilon)}{\partial t} + \frac{\partial(\rho \epsilon u_i)}{\partial x_i} = \frac{\partial}{\partial x_j} \left[\frac{\mu_t}{\sigma_\epsilon} \frac{\partial \epsilon}{\partial x_j} \right] + C_{1\epsilon} \frac{\epsilon}{k} 2\mu_t E_{ij} E_{ij} - C_{2\epsilon} \rho \frac{\epsilon^2}{k} \quad (2.27)$$

where u_i represents velocity component in corresponding direction, E_{ij} the component of the rate of deformation and μ_t the eddy viscosity:

$$\mu_t = \rho \frac{C_\mu k^2}{\epsilon} \quad (2.28)$$

The model value constants are:

$$C_\mu = 0.09, C_{1\epsilon} = 1.44, C_{2\epsilon} = 1.92, \sigma_k = 1.0, \sigma_\epsilon = 1.3 \quad (2.29)$$

To compute the Reynold stresses the Boussinesq relationship (2.30) is used.[7]

$$-\overline{\rho u'_i u'_j} = \mu_t \left(\frac{\partial U_i}{\partial x_j} + \frac{\partial U_j}{\partial x_i} \right) - \frac{2}{3} \rho k \delta_{ij} = 2\mu S_{ij} - \frac{2}{3} \rho \delta_{ij} \quad (2.30)$$

The Reynolds flux vectors for energy and species transport can be written as:

$$\overline{\rho u'_j E''} = - \frac{\mu_t}{Pr_t} \frac{\partial \tilde{E}}{\partial x_j} \quad (2.31)$$

and

$$\overline{\rho u'_j Y''_i} = - \frac{\mu_t}{Pr_t} \frac{\partial \tilde{Y}_i}{\partial x_j} \quad (2.32)$$

respectively, where Pr_t is the turbulent Prandtl number and μ_t is the turbulent viscosity.

2.1.5 Liquid Breakup and Breakup Models

The liquid fuel injection, atomization and spray formation are key in-cylinder processes that affects the combustion and emission characteristics in an internal combustion engine. To achieve cleaner and more efficient combustion processes the fuel spray characteristics and injection strategies have to be well optimised. This is to achieve better fuel evaporation, fuel/air mixing process and a more complete combustion process. In order to describe and model this fuel atomization and breakup process when using CFD simulations, different spray models has been developed [11].

KHRT Breakup Model

The KHRT breakup model introduces the competition of the droplet breakup due to Kelvin-Helmholtz aerodynamic instabilities and Rayleigh-Taylor instabilities, and the one predicting the fastest onset of an instability dominates the breakup process. In the KH breakup process, the small droplets are shed from the parent computational parcel to form a new parcel. The parent droplet with a radius larger than the wavelength of the growing unstable surface wave will break into a new parent and child droplet pair. The diameter of the stable child droplet, D_s is calculated as:

$$D_s = 2B_0 \Lambda_{KH} \quad (2.33)$$

where Λ_{KH} is the wavelength of the growing unstable surface wave and B_0 is a model constant. The standard value for the model constant B_0 is 0.61. The rate of change of the parent droplet diameter D_d is given by:

$$\frac{dD_d}{dt} = -\frac{D_d - D_{d,stable}}{\tau_{KH}} \quad (2.34)$$

where the characteristic breakup timescale τ_{KH} is calculated using:

$$\tau_{KH} = \frac{3.726B_1D_d/2}{\Delta_{KH}\Omega_{KH}} \quad (2.35)$$

where B_1 is a model constant ranging between 10 and 60. Ω_{KH} is the growth rate of the fastest growing wave. If the difference between the original and the new parcel mass is greater than a threshold, usually 3% of the of the original mass, the smaller droplets are shed off to form a new parcel [11].

In the RT breakup process, the droplet diameter D_d should be larger than the wavelength Λ_{RT} of the fastest growing wave. This is scaled by a constant C_3 with the range of 0.1-1,

$$D_d = C_3\Lambda_{RT} \quad (2.36)$$

Additionally, time greater than the RT breakup timescale, τ_{RT} must have passed since the last RT breakup. The wavelength Λ_{RT} is obtained by calculating the corresponding wave number $k_{RT} = 2\pi/\Lambda_{RT}$ which maximizes the growth rate which is given by:

$$\omega(k) = -k^2 \left(\frac{\mu_d + \mu}{\rho_d + \rho} \right) + \sqrt{k \left(\frac{\rho_d - \rho}{\rho_d + \rho} \right) a - \frac{k^3 \sigma}{\rho_d + \rho} + k^4 \left(\frac{\mu_d + \mu}{\rho_d + \rho} \right)^2} \quad (2.37)$$

where μ is ambient dynamic viscosity, μ_d is the fuel droplet dynamic viscosity, a is the acceleration or deceleration of the droplet, while:

$$\tau_{RT} = \frac{C_\tau}{\omega_{RT}} \quad (2.38)$$

$$\omega_{RT} = \omega(k_{RT}) \quad (2.39)$$

where C_τ is a model constant often set equal to 1 [11].

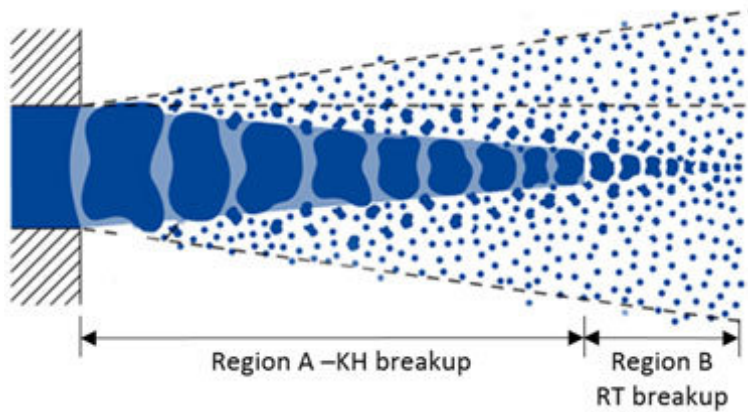


Figure 2.1: Schematic over the two break-up regions [12]

2.1.6 Rosin-Rammler Particle Size Distribution

Particle size distribution functions are used to characterize dispersed systems like powders and droplets. Often, mathematical distribution functions are fitted to size distributions to derive a specific size for parameters for such as modeling purposes. One of the most well known and popular model is the Rosin-Rammler size distribution model. The model is used in a broad range of applications ranging from biproducts development to breakup of liquid drops, aerosol technology, meteorology and more. Furthermore, the model is used to characterize seed size and to investigate the influence of the particle size distribution on the minimum ignition energy of explosive dusts [13].

The Rosin-Rammler distribution function is generally given in the cumulative-volume form:

$$V = 1 - R = 1 - \exp\left(-\left[\frac{x}{x'}\right]^n\right) \quad (2.40)$$

where:

V = mass or volume fraction of particles with sizes smaller than or equal to x (= undersize distribution), assuming constant mass density of all particles.

R = mass or volume fraction of particles with sizes larger than x (= oversize distribution).

x = particle size ($x \geq 0$) expressed in, e.g., μm

x' = location parameter of the distribution, i.e., the particle size at a volume fraction of 0.368 oversize ($x' \geq 0$)

n = spread parameter of the distribution ($n \geq 0$)

The volume density distribution of the Rosin-Rammler distribution can be obtained by differentiation of equation 2.40:

$$dV/dx = \frac{n}{x'} \left(\frac{x}{x'}\right)^{n-1} \exp\left(-\left[\frac{x}{x'}\right]^n\right) \quad (2.41)$$

In OpenFOAM, the particle size distribution model draws random sample from the doubly-truncated two-parameter Rosin-Rammler probability density function:

$$f(x; \lambda, n, A, B) = \frac{\frac{n}{\lambda} \left(\frac{x}{\lambda}\right)^{n-1} \exp\left[-\left(\frac{x}{\lambda}\right)^n\right]}{\exp\left[-\left(\frac{A}{\lambda}\right)^n\right] - \exp\left[-\left(\frac{B}{\lambda}\right)^n\right]} \quad (2.42)$$

where:

λ = Scale parameter

n = Shape parameter

x = Sample

A = Minimum of the distribution

B = Maximum of the distribution

Random samples are generated by the inverse transform sampling technique by using the quantile function of the doubly-truncated two-parameter Rosin-Rammler (Weibull) probability density function:

$$x = \lambda(q_{min} - \ln(1 - ur))^{1/n} \quad (2.43)$$

with

$$r = 1 - \exp(-q_{max} + q_{min}) \quad (2.44)$$

$$q_{min} = \left(\frac{A}{\lambda}\right)^n \quad (2.45)$$

$$q_{max} = \left(\frac{B}{\lambda}\right)^n \quad (2.46)$$

where u is a sample drawn from the uniform probability density function on the unit interval (0,1) [14].

2.2 Liquefied Petroleum Gas

Liquefied petroleum gas (LPG), also known as propane autogas, is a clean burning alternative fuel used in light- and heavy duty propane vehicles. Propane is considered a good, more environmentally friendly alternative to traditional fuels such as gasoline and diesel [15]. Due to having a much higher hydrogen:carbon monoxide ratio than diesel and gasoline, greenhouse gas emissions can be significantly reduced if an equivalent energy conversion can be achieved when using LPG. Furthermore, propane presents no threat to soil, surface water or groundwater if spilled [16]. The high octane rating of propane, together with a high flame speed, makes it a very good choice in spark-ignited internal combustion engines with a research octane number rating of up to 105 compared to gasoline with a rating of 84-93 [17]. Compared to compressed natural gas which has an energy density of 9 MJ/L @ 248 Bar, stored as a liquid, LPG is stored as a liquid at more moderate pressures and temperatures at the same time as it has a higher energy density, ~ 27 MJ/L @ 24 Bar [18].

2.2.1 Flash Boiling

Limiting factors to achieve high efficiency in engines involve engine knock, misfires, low emissions limits and the wide range of chemical reactivity in LPG. An important factor that also needs to be taken into account when using LPG as working liquid is the flash-boiling effect. Propane, that is the main component of LPG, is prone to flash-boiling at normal GDI engine operating conditions compared to traditional fuels. This is something that needs to be taken into account due to the fact that the phenomenon will lead to drastic change in the spray's behaviour.

Flash-boiling is a phenomenon that occurs when a sub-cooled liquid is rapidly depressurized to a pressure sufficiently below the saturation point of the liquid. In this state, the fuel is defined as superheated and the system is in a state of thermodynamic non-equilibrium and thus unstable. To regain the equilibrium in the system, flash boiling occurs [19].

The flash boiling mechanism can be defined into three stages, namely: Bubble Nucleation, Bubble Growth and Two-phase flow. Bubble Nucleation is classified into two groups: Homogeneous and Heterogeneous. Homogeneous nucleation is when nucleation sites form within the liquid itself with a homogeneous distribution. This becomes predominant when the liquid pressure is considerably reduced. Heterogeneous nucleation occurs when gas and solid phases appear at an interface or a body, not in the liquid. A nucleus can appear in the presence of irregularities on a solid surface, fine dust or solid particles and dissolved gases in the liquid [19].

When the bubble nucleation sites have developed, pressure fluctuations can cause the sites to either collapse or grow. Whilst the bubble still is relatively small, the rate of growth is low and restricted by the bubbles surface tension. However, if the degree of superheat is great enough, the growth rate reaches a maximum as the size of the bubble increases. The liquid surrounding the bubble is then cooled due to the transfer of heat energy required for evaporation, with this, the vapor pressure decreases and bubble growth rate is controlled by inertia and thermal diffusion. Following this, the bubble growth rate further decreases and inertial effects become less important. At this stage the growth rate is controlled by thermal diffusion. The growth then stop when the bubble interior pressure and temperature approach ambient values [19].

The growth of bubbles inside a droplet is limited. A limit determined by the diameter of the droplet, surface tension, liquid viscosity, the number density of bubble nuclei and growth rate. The limit of bubble growth is described by the void fraction, ϵ , defined as the volume ratio between the vapor and liquid phases:

$$\epsilon = \frac{V_{bubble}}{V_{bubble} + V_{liquid}} \quad (2.47)$$

where V_{bubble} is the volume of bubbles and V_{liquid} is the volume of liquid. In a study by S.Suma and M. Koizumi [20], it has been observed that break up of a jet fuel occurs at ϵ ranging from 0.51 to 0.53 [21]. After this it is assumed that the droplet breaks up into small droplets twice as many as the number of bubbles, this is illustrated in figure 2.2.

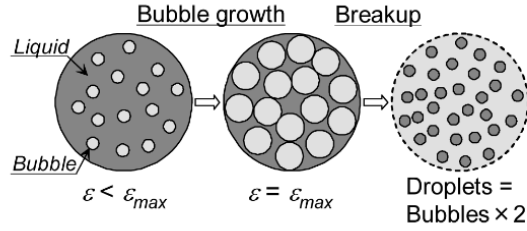


Figure 2.2: Break up cause by bubble disruption [21]

The momentum of the parent droplet is uniformly distributed among the child droplets. Once the flash boiling process is completed a two-phase flow consisting both of fluid and vapour in equilibrium is obtained.

2.3 Design of Experiment

To understand cause and effect relations in a system the input variables to the system have to be deliberately changed. These changes in the output from the system must then be observed. That is to say, an experiment needs to be performed on the system.

Experiments are conducted on all types of questions regarding a system and its processes. An experiment can be defined as a test or series of runs in which purposeful changes are made to the input variables of a process or system. Doing this, one may observe and identify the reasons for changes that may be seen in the output response [22]. When conducting these experiments one might want to determine which variables are responsible for the observed change in output response from the system, develop a model that relates the response to the important input variables and use this model to help improve and ease the decision making regarding the system.

Experiments and experimentation is an important engineering method and is a vital tool when examining how and why a system works the way it does. A well designed experiment is important due to the fact that the results and conclusions that are drawn from the tests depends greatly in the manner the data was collected [22].

2.3.1 2^k Factorial Designs

Factorial experiment designs are used to great extent in experiments involving several factors where it is necessary to study the combined effect of the factors on a response. There are a number of special cases of the general factorial design that are widely used in research work. The most important case is the one of k factors where each factor only has two levels. The levels may be quantitative, such as temperature or pressure or they may be qualitative, such as number of workers or the presence of absence of a factor. To replicate such a design $2 * 2 * 2 \dots * 2 = 2^k$ observations are required. This is called a 2^k factorial design [22].

The simplest 2^k factorial design is the 2^2 design, in this case there are two factors A and B that has two levels each. This means that 4 runs are made where several (n) replications are taken. The lowercase letters a, b, ab and (1) is used to indicate the sum of the responses for all replications of A and B levels. If the lowercase letter is present the factor is at its high (+1) level. If it does not appear the factor is at its lower level (-1).

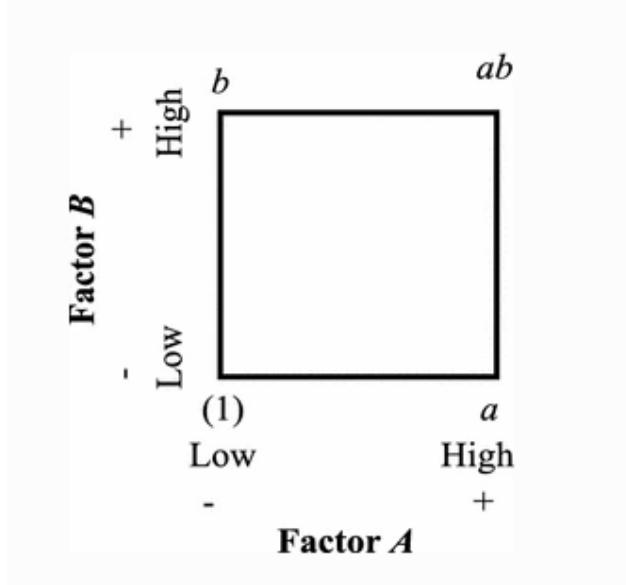


Figure 2.3: Geometrical view of 2^2 factorial design [23]

Factor Level Combinations	Coded Levels	Replicate				Sum of n Replicates	
		1	2	...	n		
A low, B low	-1 -1	xxx	xxx	...	xxx	(1)	$=y_{11}$
A high, B low	+1 -1	xxx	xxx	...	xxx	a	$=y_{21}$
A low, B high	-1 +1	xxx	xxx	...	xxx	b	$=y_{12}$
A high, B high	+1 +1	xxx	xxx	...	xxx	ab	$=y_{22}$

Table 2.1: Data in a general 2^2 factorial experiment

The average effect factor is the average change in the response produced by a change in the level of that factor averaged over the levels of the other factor [24]. For a general 2^2 design with n replicates the main effect factor for A, denoted by A, is:

$$A = \frac{1}{2n}([ab - b] + [a - (1)]) = \frac{1}{2n}[ab + a - b - (1)] \quad (2.48)$$

here the effect of A at the low level of B, $[a - (1)]/n$, and the effect of A at the high level of B, $[ab - b]/n$, are averaged yielding the main effect of A. The same principle is used for finding the main effect of B. Here the effect of B at a low level of A, $[b - (1)]/n$ are averaged with the effect of B at a high level of A, $[ab - a]/n$

$$B = \frac{1}{2n}([ab - a] + [b - (1)]) = \frac{1}{2n}[ab - a + b - (1)] \quad (2.49)$$

The symbols (1), a, b and ab represent the total of the response variable at all n replicates taken at the factor level combinations.

The interaction effect, denoted as AB, is defined as the average difference between the effect of A at the high level of B and the effect of A at the low level of B:

$$AB = \frac{1}{2n}([ab - b] - [a - (1)]) = \frac{1}{2n}[ab + (1) - a - b] \quad (2.50)$$

The interaction effect could also be defined as the average difference between the effect of B at the high level of A and the effect of B at the low level of A. This would also lead to equation 2.50 [22].

In order to determine the importance of each variable, it is essential to examine the magnitude and direction of the factor effects when working with 2^k designs. To determine the importance of a variable, analysis of variance, ANOVA, can be used together with effect magnitude and direction. One way of determining the importance is the sums of squares together with an ANOVA.

To determine the sums of squares for A , B and AB one can look at equation 2.48 where a contrast is used for estimating A , specifically

$$C_A = ab + a - b - (1) \quad (2.51)$$

This contrast is often called the total effect of A . Equations 2.49 and 2.50 illustrates that contrast are also used to determine B and AB . Additionally, these three contrasts are orthogonal. The sum of squares for an arbitrary contrast can be calculated with

$$SS_C = \frac{\left(\sum_{i=1}^a c_i \bar{y}_i\right)^2}{\frac{1}{n} \sum_{i=1}^a c_i^2} \quad (2.52)$$

where \bar{y}_i is the observed sample mean.

This equation states that the sum of squares for any contrast is equal to the contrast squared divided by the number of observations in each total in the contrast times the sum of the squares of the contrast coefficients [22]. This yields the following sums of squares for A , B and AB

$$SS_A = \frac{[ab + a - b - (1)]^2}{4n} \quad (2.53)$$

$$SS_B = \frac{[ab + b - a - (1)]^2}{4n} \quad (2.54)$$

and

$$SS_{AB} = \frac{[ab + (1) - a - b]^2}{4n} \quad (2.55)$$

With the help of these equations together with the ANOVA one can conclude which factors are significant and if there are any interactions between the different factors. The same principle is used for designs with $k > 2$. If, for example $k = 3$, factors A , B and C will be present.

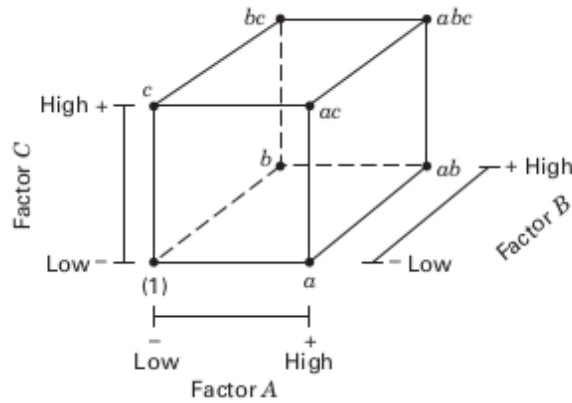


Figure 2.4: Geometric view for a 2^3 factorial design [22]

2.3.2 Space Filling Designs

The use of computer simulations are rapidly increasing and the large computational power that is available today makes it possible to simulate large and complex systems. The results from these simulations are most often deterministic. This means that the computer experiment always will produce the same results if the input parameters are not changed. This means that there is little to no noise in the response. In classic designs, such as in 2^k factorial designs, randomization, replication and blocking are three foundations that are emphasised when selecting a specific design. These principles are however irrelevant for deterministic models since the response will always be the same for that specific factor combination. Replicates in these cases waste resources. Due to the deterministic output from computer experiments, the models often require higher order terms. These terms are needed for tests in order to understand the properties of the true physical system. For these reasons, closing just the corner points as in factorial designs is not enough [25].

To fill the design space, space filling designs can be used. In these designs the design points are spread out evenly in the design region. It is to note that an important assumption is necessary to use in these models: the computer simulation must reflect the true physical system. The space filling designs are able to capture the different behaviours of responses in different areas of the design region due to the spread out points. These designs do not seek to have replicates in k dimensions, where k is the number of factors. If factors are found with no statistical effect on the response and the dimension of the design space is reduced as a reaction to it, the design will not have replicate points in the lower dimension design space. This allows the user to gain more information about the system. This is because replicated test points do not provide additional information and the response is deterministic [25].

Metrics that are meaningful for classical designs such as power, prediction variance and the alias properties of the design, is no longer meaningful for deterministic designs. Instead space filling design use metrics as minimum distance between points and discrepancy. If the sample size is fixed, the larger the minimum distance is the better. The discrepancy measures how evenly the points are spread out throughout the design region, the smaller discrepancy the better [25]. There are several space filling designs used, the one used and discussed in this report is the Latin Hypercube Design.

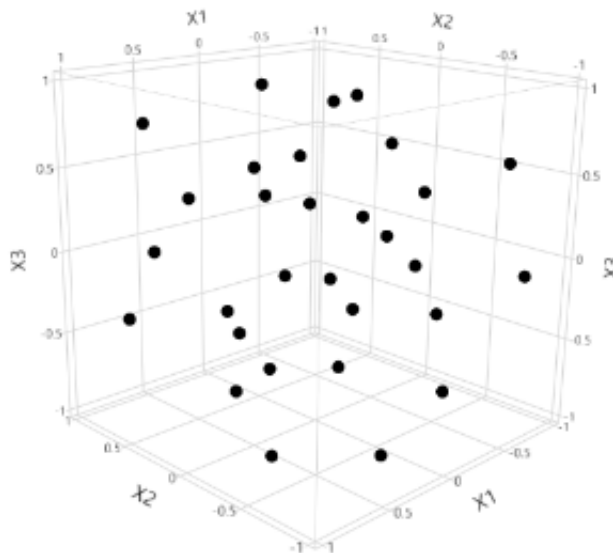


Figure 2.5: Latin Hypercube Design for three factors [25]

The Latin Hypercube design select design points with the objective to maximize the minimum distance

between design points, but requires the design points to be evenly spaced in the design space. The design also requires all factors to be continuous. The design is one of the most popular designs and used in practice due to its balanced nature. The design is effective when trying to capture the different behaviours of responses in different regions of the design space. The Latin hypercube design is the model that best captures the design region due to the fact that it selects points both on the limits and in the center of the design region. An important thing to note however is that the model does not work when using categorical factors [25].

2.3.3 Analysis Of Variance Tests

To analyse results from conducted experiments, an Analysis of variance, ANOVA, test can be conducted. For conducting the ANOVA test, there has to be collected data regarding at least one categorical independent variable, parameter, and one quantitative dependent variable, response. The independent variable should also have levels, such as high and low. Each level creates a group [26].

The ANOVA test determines if these groups, created by the different levels, are statistically different by calculating the mean of the levels and seeing if these are different from the overall mean of the dependent variable. If any of the means from the groups are significantly different from the overall mean, the null hypothesis is rejected and thus the levels has an effect on the response [26].

For calculating statistical significance, the ANOVA uses an F-test. This test allows for multiple comparisons of means at once. The F-test takes the variance in each group mean and compares it to the overall group variance. If the variance within the groups are smaller than the variance between the groups, the F-test will find a higher F-value. The higher the F-value, the higher the likelihood that the difference observed is real and not due to chance [26].

Chapter 3

Method

3.1 Method Overview

A model and geometry was created to simulate the injection of LPG into a closed chamber using OpenFOAM. The setup was based on the aachenBomb tutorial found in OpenFOAM using the sprayFoam solver. This tutorial was altered by using a modified geometry together with changed fuel and injection properties. The injector profile was chosen to be the standard "Spray G" injector profile from the Engine Combustion Network [27]. Setup parameters for the simulations were collected from the paper "Bulk Spray and Individual Plume Characterization of LPG and Iso-Octane Sprays at Engine-Like Conditions" by B. Windell and M. Sharma [18], where LPG was injected into a high pressure spray chamber and evaluated using high-speed Schlieren Imaging and Planar Mie Scattering Imaging [18]. The experimental results were collected from Windell et.al [18] by extracting the values from the plots using a web based tool called WebPlotDigitizer. These values were then used to validate the results obtained from the CFD-simulations.

After the CFD-setup was finalized, it was used for the simulations created by the DoE models. Two models were created using the open source software Rstudio, based on the R programming language, with four parameters analyzed. The first model was a 2^4 factorial design consisting of 16 runs, the second one was a Latin hypercube design also consisting of 16 runs. The two models were created using the SixSigma [28] and MaxPro [29] R-packages, respectively. The responses from the simulations were then examined and comparisons using ANOVA tests between the two models were performed.

3.2 CFD-Case Setup

3.2.1 Geometry

The geometry used for the simulation was a 3D "slice" with an angle at the tip of 45 degrees, this represents $\frac{1}{8}$ of a cylindrical domain with a "Spray G" injector at the top. Due to the symmetric nature of the "Spray G" injection profile only one of the eight holes was simulated with cyclic boundary conditions at the adjacent walls. The geometry is shown in figure 3.1 below.

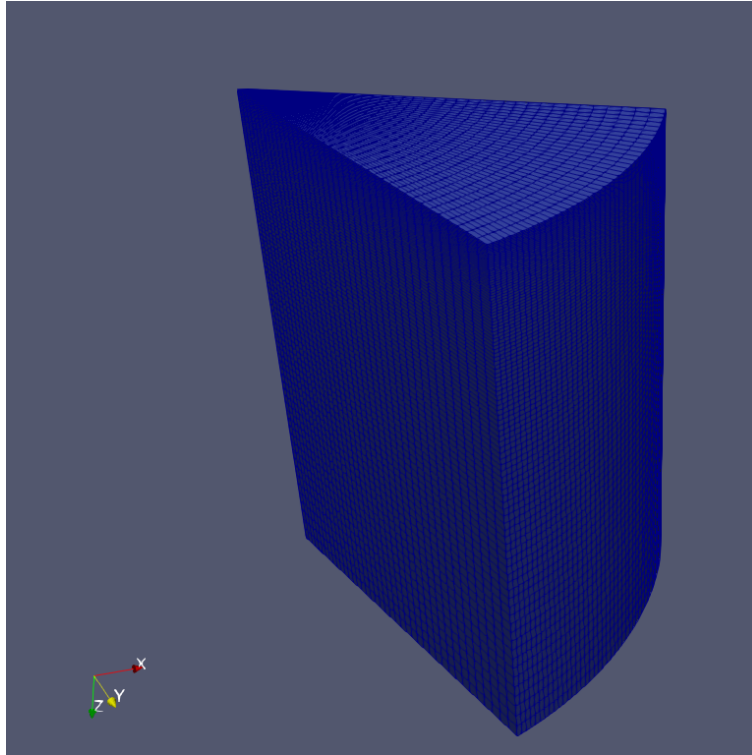


Figure 3.1: Slice shaped geometry

The geometry had a height of 100 mm and a radius of 75 mm . A schematic of the geometry can be seen in figure 3.2. To remove the risk of meshing problems near the point of the slice, the tip of geometry was cut off. The injector was placed in the middle of the slice located 0.40 mm from the rear cut off with an injection angle of 37 degrees as specified in the Engine Combustion Network [30]. The injector orifice had a diameter of 0.165 mm .

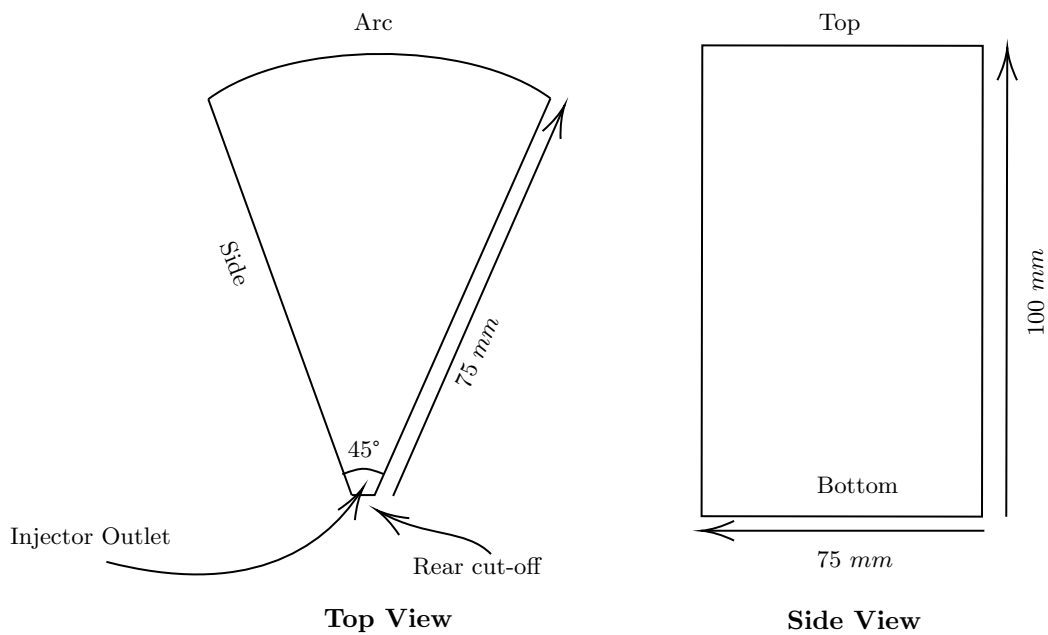


Figure 3.2: Schematic view of the geometry

3.2.2 Spray G Injection Profile

As stated earlier, the injection profile for the injector used was the standard Spray G configuration from the Engine Combustion Network. The injector specification for this case are for modern advanced injection systems with high pressure capability [27]. The specified geometry specification for the injector is described in table 3.1 and figure 3.3.

Number Of Holes	8
Spray Shape	Circular
Bend Angle	0°
L/D Ratio	1.4
Hole Shape	Straight
Manufacturing	EDM
Flow rate	15 cc/s @10 MPa
Fuel injector	Delphi solenoid-activated
Nozzle type	Valve-covered orifice
Nozzle shape	Step hole
Orifice diameter	0.165 mm
Orifice length	0.16-0.18 mm
Step diameter	0.388 mm
Orifice drill angle	37° relative to nozzle axis
Fill outer spray angle	80°

Table 3.1: Specifications for standard Spray G geometry [30]

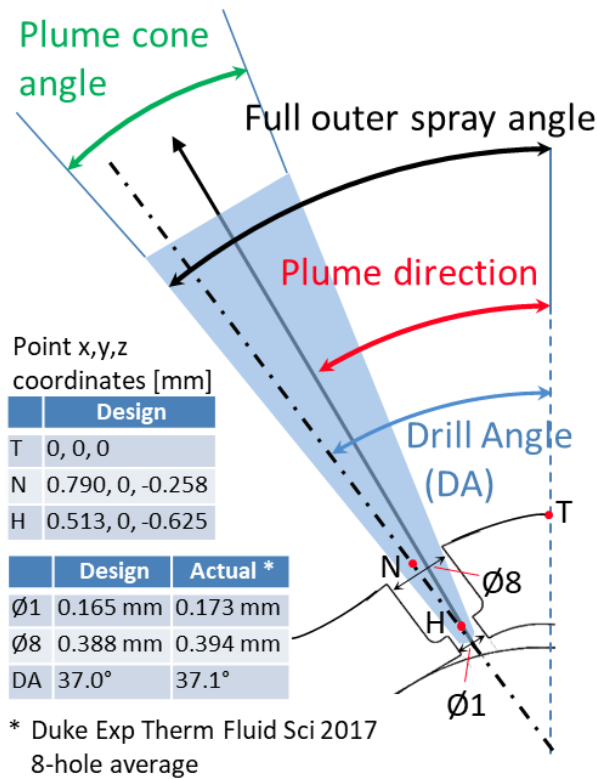


Figure 3.3: Specified geometry for Spray G [30]

3.2.3 Boundary And Initial Conditions

The boundary conditions for each boundary are specified in table 3.2. Due to the symmetric nature of the problem, the side walls were specified as cyclic where the two sides had the opposite side as neighbour patch i.e. the right side had the left side as neighbour patch and vice versa for the left side.

Region Boundary	Boundary Condition
Top	No slip, Wall
Bottom	No slip, Wall
Arc	No slip, Wall
Rear cut-off	No slip, Wall
Sides	Cyclic, Wall

Table 3.2: Boundary conditions

Several different cases for the initial conditions were explored in the paper by Windell et.al [18]. The initial conditions utilized for the simulations were the so called G3C conditions, these conditions are listed in table 3.3. The G3C conditions represent part-load, throttled, early injection conditions in a direct injection engine cylinder. For all cases 100 % liquid propane was injected into air.

Due to the fact that the mass injected in [18] was not specified, the injection velocity for the propane was calculated using Bernoulli's equation.

$$P_1 + \frac{1}{2}\rho v_1^2 + \rho g h_1 = P_2 + \frac{1}{2}\rho v_2^2 + \rho g h_2 \quad (3.1)$$

Neglecting elevation differences and assuming $v_1 = 0$, equation 3.1 can be rearranged to calculate the inlet velocity v_2 as:

$$v_2 = \sqrt{\frac{2(P_1 - P_2)}{\rho}} \quad (3.2)$$

With an injection pressure, P_1 , equal to 200 Bar, an ambient pressure in the domain of 1 Bar and a propane density of 538.07 kg/m^3 the calculated inlet velocity to the domain is $v_2 = 272 \text{ m/s}$. Assuming some pressure losses in the injector, the injection velocity was set to 250 m/s .

Fuel	Propane
Ambient Temperature [K]	293
Ambient Pressure [Bar]	1
Fuel Temperature [K]	293
Injection Pressure [Bar]	200
O_2 Concentration Chamber	23.4%
N_2 Concentration Chamber	76.6%
Injection Duration [μsec]	870
Injection Velocity [m/s]	250
Injector Orifice Diameter [mm]	0.165

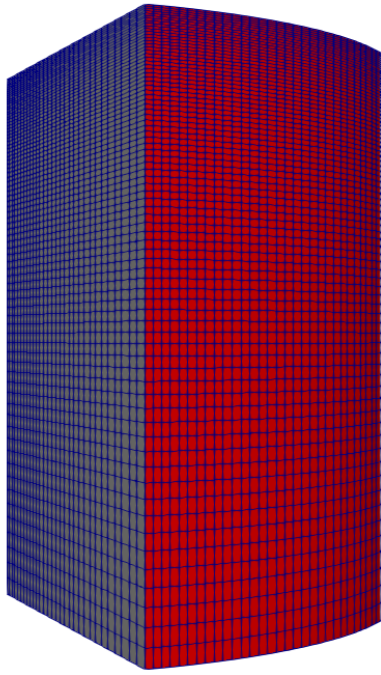
Table 3.3: Initial conditions for G3C test conditions

3.2.4 Mesh

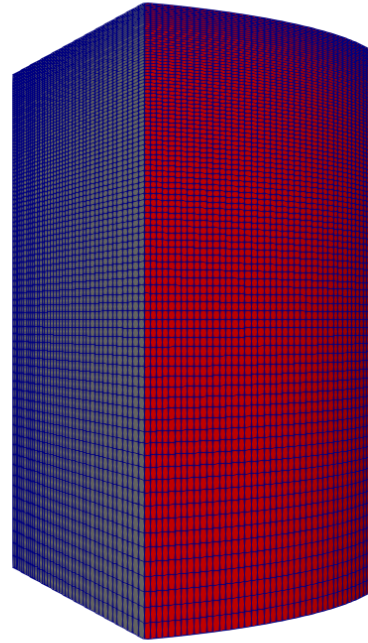
To create the mesh for the domain, the BlockMesh utility in OpenFOAM was used. This utility creates a mesh consisting of three dimensional hexahedral blocks. To reduce computational times the mesh had a grading where the mesh had the highest element density close to the injector and a gradual density decrease the further away from the injector we get. Four different meshes were created and simulated for the mesh independence study, the specifications for these can be seen in table 3.4. The mesh used has to be refined enough to capture all the important aspects of the spray behaviour such as liquid breakup and more. Furthermore, it must have reasonable computing times as the Design Of Experiment, explained later in the thesis, requires a large number of simulations to be performed.

Case	Number Of Cells	Number Of Cells In Each Direction
Coarse Mesh	72000	(30 30 80)
Base Mesh	160000	(40 40 100)
Fine Mesh	540000	(60 60 150)
Even Finer Mesh	1152000	(80 80 180)

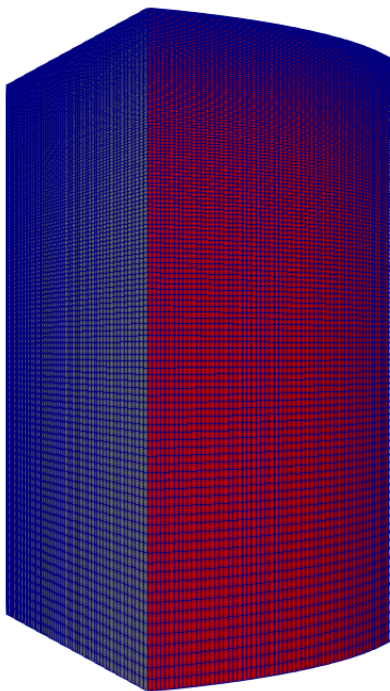
Table 3.4: Grids generated for mesh independence study



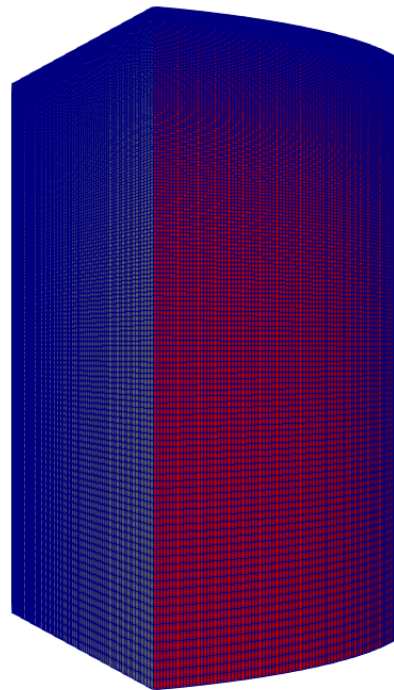
(a) Coarse Mesh



(b) Base Mesh



(c) Fine Mesh



(d) Even Finer Mesh

Figure 3.4: Grids generated for mesh independence study

3.2.5 Mesh Sensitivity Analysis

The four different meshes were simulated and evaluated using the settings and initial conditions presented in table 3.3. The parameters evaluated for the mesh sensitivity was maximum liquid penetration length and maximum vapor penetration length in the domain over the first 1200 microseconds after injection. The liquid penetration was defined as where the spray contained 95 % of the original mass of the liquid injected into the domain. For the vapor penetration, if the mass fraction of fuel compared to air was greater than 1 percent it was used in the calculation for vapor penetration.

The comparisons showed that the fine mesh consisting of 540 000 cells is the optimal choice. It can be seen that the solution is converging as the deviation in the results between the two finest meshes are at a maximum 2.5% when looking at the liquid penetration in figure 3.5. When looking at the vapor penetration, the difference between the two meshes are even smaller at a maximum of 1.2%, figure 3.6. As the differences between the two finer meshes are so small, it was decided to use the finer mesh consisting of 540 000 cells. This mesh is sufficiently accurate to capture all important aspects of the spray as at the same time it yields reasonable computing times, something that is key for the design of experiment analysis.

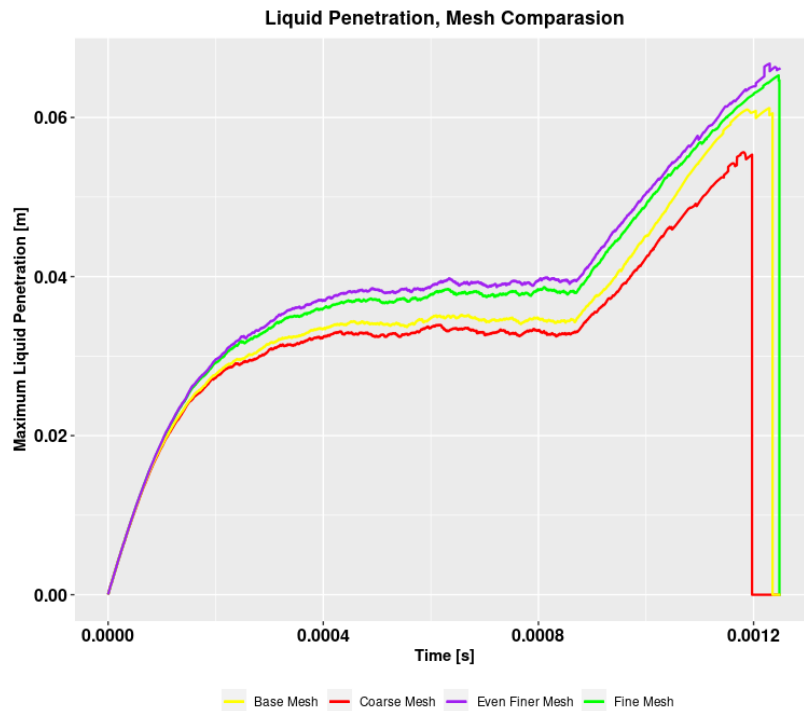


Figure 3.5: Maximum liquid penetration between the simulated grids

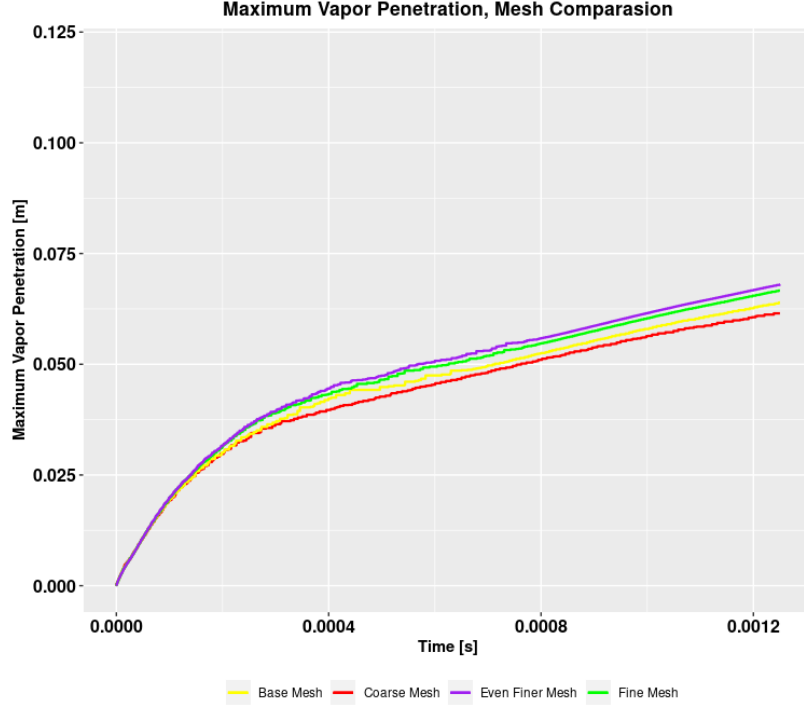


Figure 3.6: Maximum vapor penetration between the simulated grids

3.2.6 Model Parameter Analysis

To see how the parameters in the KHRT breakup model changed the results in the CFD simulations a number of simulations with different values of the B0 and B1 parameters was performed. The point of this exercise was to see if a higher correlation with the experimental results could be achieved. In total 7 simulations was performed, the input for the breakup parameters are shown in table 3.5. The base values used were collected from the aachenBomb tutorial in the OpenFOAM environment.

Run Number	B0 Value	B1 Value
1, Base	0.61	40
2	0.1	40
3	0.2	40
4	1	40
5	0.61	10
6	0.61	20
7	0.61	60

Table 3.5: KHRT breakup parameter values used for comparison

As for the KHRT parameters, the parameters in the Rosin-Rammler function was examined and changed. The goal with this was also to see how the parameters changed the simulation results and to see if the correspondence with the experimental results could increase. The values used can be seen in table 3.6. Also here the base value was collected from the aachenBomb tutorial.

Run Number	maxValue	d Value
1, Base	0.00015	0.00015
2	0.00005	0.00005
3	0.00010	0.00010

Table 3.6: Rosin-Rammler parameter values used for comparison

Simulations with the base values are represented in purple in the figures below.

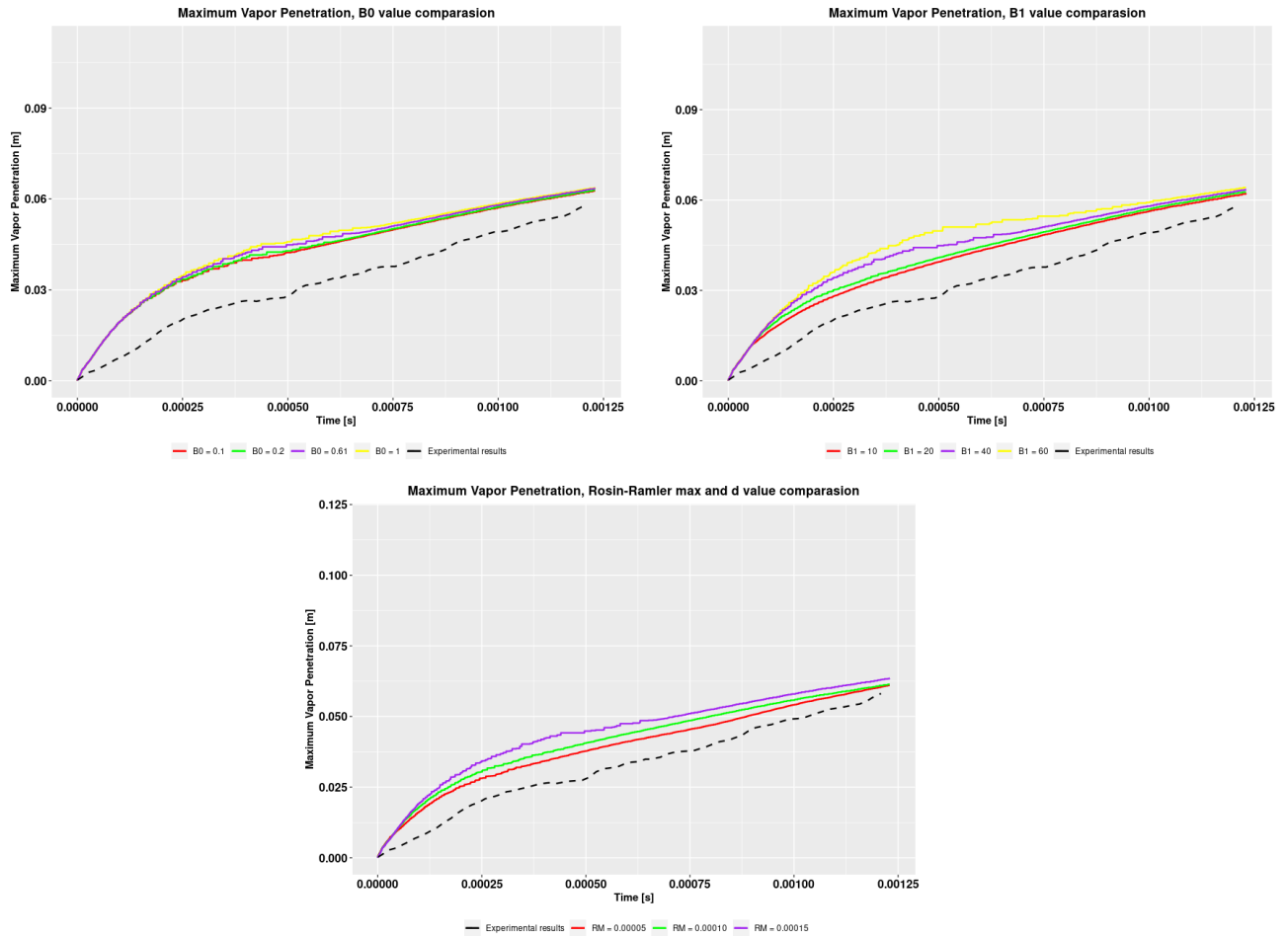


Figure 3.7: Maximum vapor penetration with changed model parameters

The results show that the change of parameters, both in the KHRT breakup model and the Rosin-Rammler particle size distribution model, translates the vapor penetration and liquid penetration curves up or down. When increasing the B0 and B1 value the curves both for the liquid and vapor penetration heightens, increasing the penetration length. However, for the vapor penetration, the parameter values does not affect the results as significant as it does for the liquid penetration. For the liquid penetration we can see large differences, especially when changing the B1 and Rosin-Rammler parameters. Increasing the parameter values moves the curve higher up, but it still maintains the same profile.

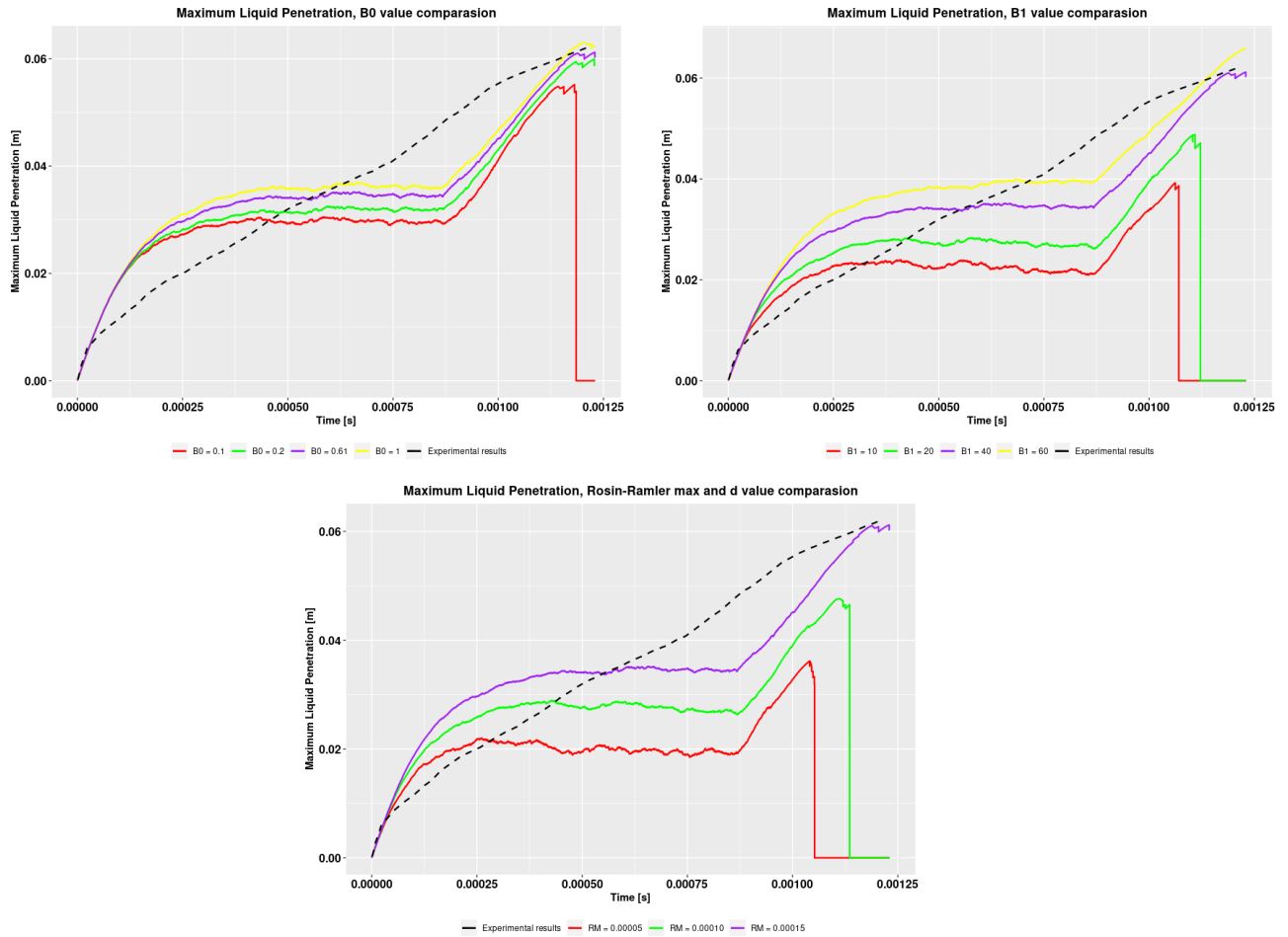


Figure 3.8: Maximum liquid penetration with changed model parameters

Decreasing Rosin-Rammler and B1 parameters showed a good potential for increasing the accuracy of the vapor penetration length, moving the curve downwards towards the experimental results. However, when decreasing these values the curves for the liquid penetration also moved downwards, decreasing the accuracy by moving the curves further away from the experimental results. As the change of parameter values did not show any clear or significant improvements, it was decided to use the base values of $B0 = 0.61$, $B1 = 40$ and $RM = 0.00015$ for all the simulations conducted for this thesis.

3.3 Design Of Experiment Setup

For creating and analyzing the Design of Experiments, the software Rstudio was used. Both a 2^k factorial and Latin Hypercube design was constructed using Rstudio and then simulated with the specified parameter values from the DoE designs. For the DoE four parameters were considered; Injector Orifice Diameter, Injection Magnitude, Chamber (Ambient) Pressure and Chamber Temperature. All parameters were considered to be continuous with an infinite number of values between a set range of two extreme values for the Latin Hypercube model, the extreme value for each parameter is presented in table 3.7.

Parameter	Minimum Value (-)	Maximum Value (+)
Injector Orifice Diameter [mm]	0.100	0.300
Injection Magnitude [m/s]	100	300
Chamber Pressure [Bar]	1	50
Chamber Temperature [K]	293	700

Table 3.7: Minimum and maximum values for parameters in DoE

For the DoE it was decided to run 16 simulations, i.e. there would be 16 points in the Latin Hypercube. This decision was made to try to get a more accurate way of comparing the Latin Hypercube and 2^k factorial designs. With 16 runs, there is an equal number of runs for the two different models.

Two main responses were examined for the two different models: Vapor penetration at 870 μs , i.e. at the end of injection and Liquid penetration at 870 μs .

3.3.1 2^4 Factorial Design

The factorial design was created using the SixSigma package available in RStudio. The design is a full factorial meaning that all 16 combinations of the 4 factors are accounted for. Each factor has a high and a low value where all of these values are combined to create 16 cases. The parameter values and combinations for each of the 16 runs is shown in table 3.8.

To be able to linearly fit the model and perform analysis on the response, replications for each run had to be made. However, as computer experiments are deterministic, the replications were assumed to have the same response values as the first 16 simulations. The two responses for each of the 16 runs were then aggregated. Aggregating these results however just resulted in the same original response for each run, as expected. The reason for this is that the SixSigma package requires replicates to function correctly.

To see which factors were significant and affected the results, the effect of the factors were examined together with the interaction between the factors. Furthermore, ANOVA tests were conducted to examine the results.

Run Number	Injector Diameter [m]	Injection Magnitude [m/s]	Chamber Pressure [Pa]	Chamber Temperature [K]
1	1E-04	100	1E+05	293
2	3E-04	100	1E+05	293
3	1E-04	300	1E+05	293
4	3E-04	300	1E+05	293
5	1E-04	100	5E+06	293
6	3E-04	100	5E+06	293
7	1E-04	300	5E+06	293
8	3E-04	300	5E+06	293
9	1E-04	100	1E+05	700
10	3E-04	100	1E+05	700
11	1E-04	300	1E+05	700
12	3E-04	300	1E+05	700
13	1E-04	100	5E+06	700
14	3E-04	100	5E+06	700
15	1E-04	300	5E+06	700
16	3E-04	300	5E+06	700

Table 3.8: Parameter values used for runs made by the 2^4 factorial design

3.3.2 Latin Hypercube Design

The Latin hypercube design was created using the MaxProLHD function in the MaxPro package in RStudio. To match the number of runs as the factorial design, it was chosen to create 16 runs. The function created 16 runs where the minimum distances between the points are maximized at the same time as they are evenly distributed in the design domain. The function creates points between $[0,1]$ and distributes them in the domain. The distribution of the points for all factors in the design domain is shown in figure 3.9.

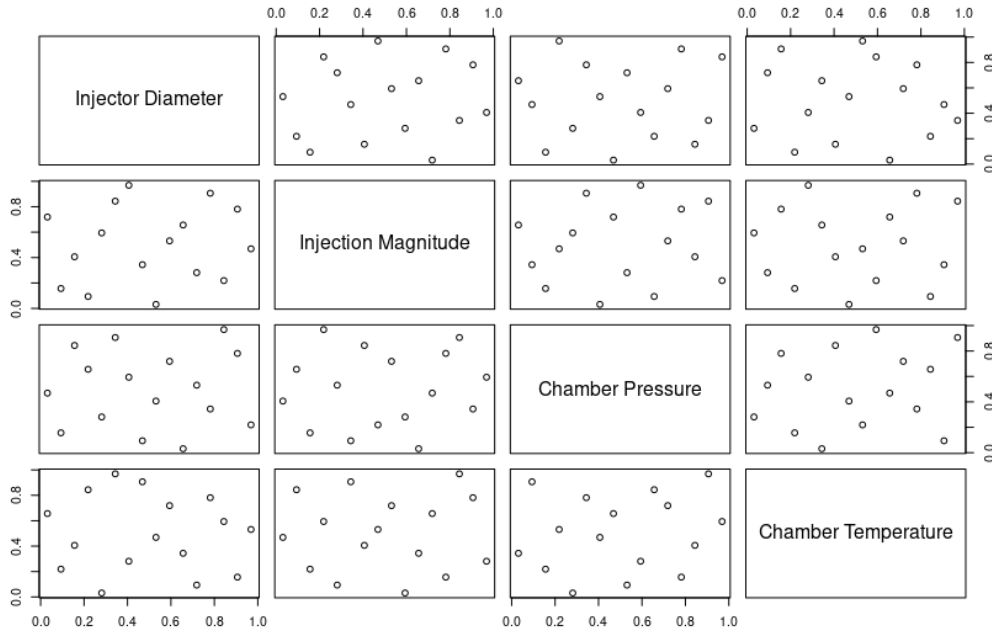


Figure 3.9: Distribution of points for all factors in the design domain for the Latin hypercube design

The points in the created design were then multiplied with a linear expression created for each factor. These expressions scaled up the points in the design domain, transforming them in such a way that the values for each factor was placed in between the minimum and maximum values presented in table 3.7. The design points after the transformation is listed in table 3.9.

Run Number	Injector Diameter [m]	Injection Magnitude [m/s]	Chamber Pressure [Pa]	Chamber Temperature [K]
1	1.031E-04	190.625	3.896E+06	429.541
2	1.156E-04	240.625	2.315E+06	578.691
3	1.281E-04	153.125	1.683E+06	330.107
4	1.406E-04	203.125	4.192E+05	528.974
5	1.531E-04	140.625	3.264E+06	678.124
6	1.656E-04	290.625	1.367E+06	628.407
7	1.781E-04	265.625	4.528E+06	379.824
8	1.906E-04	103.125	1.999E+06	479.257
9	2.031E-04	165.625	4.844E+06	553.832
10	2.156E-04	215.625	2.631E+06	305.249
11	2.281E-04	253.125	1.031E+05	454.399
12	2.406E-04	128.125	7.352E+05	603.549
13	2.531E-04	228.125	4.212E+06	653.266
14	2.656E-04	115.625	3.580E+06	354.966
15	2.781E-04	278.125	2.948E+06	504.116
16	2.906E-04	178.125	1.051E+06	404.682

Table 3.9: Parameter values used for runs made by the Latin Hypercube design

To examine the results from the simulations using the Latin hypercube parameters, ANOVA tests were conducted. This also give an opportunity to compare the two DoE models and their predictions. In addition to the ANOVA tests, 3D contour plots were created to give a visualization of how the response changes with the factors.

Chapter 4

Results

4.1 CFD Results

The results from the simulations were visualized using Paraview and RStudio to generate the line plots showing maximum vapor penetration and maximum liquid penetration. All results shown used the initial and ambient conditions described in table 3.3.

Figure 4.1 and 4.2 shows the maximum liquid and maximum vapor penetration respectively. The results show a maximum liquid penetration of 63 mm, 1200 μ s after the start of injection and a maximum vapor penetration of 67 mm after the same amount of time. The results show a quite good correlation when looking at the value of the maximum liquid penetration at 1200 μ s. However, the actual profile of the injection does not correlate very well with a large overshoot, then dropping off to undershoot before reaching the correct penetration length.

The vapor penetration maximum value does not correlate as well as the liquid penetration. Here the injection is too powerful in the beginning translating the curve upwards, this is then present during the whole sample period. However, when looking at the actual profile of the plot, it can be seen that the simulated results follows the experimental results quite good but with a constant overshoot induced in the beginning.

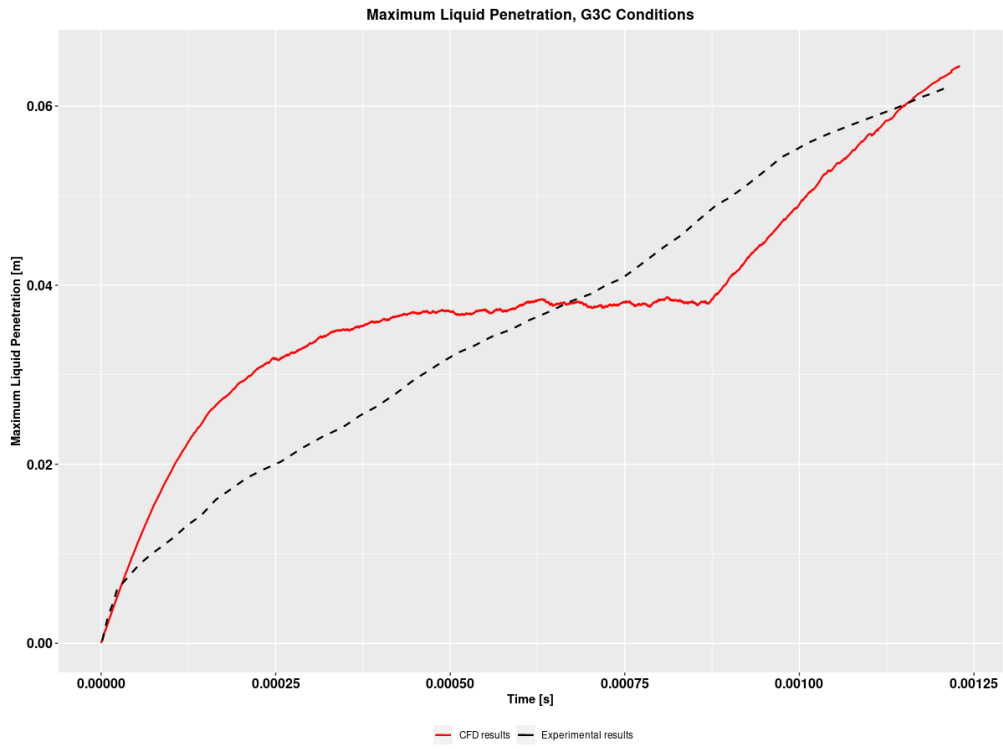


Figure 4.1: Maximum liquid penetration

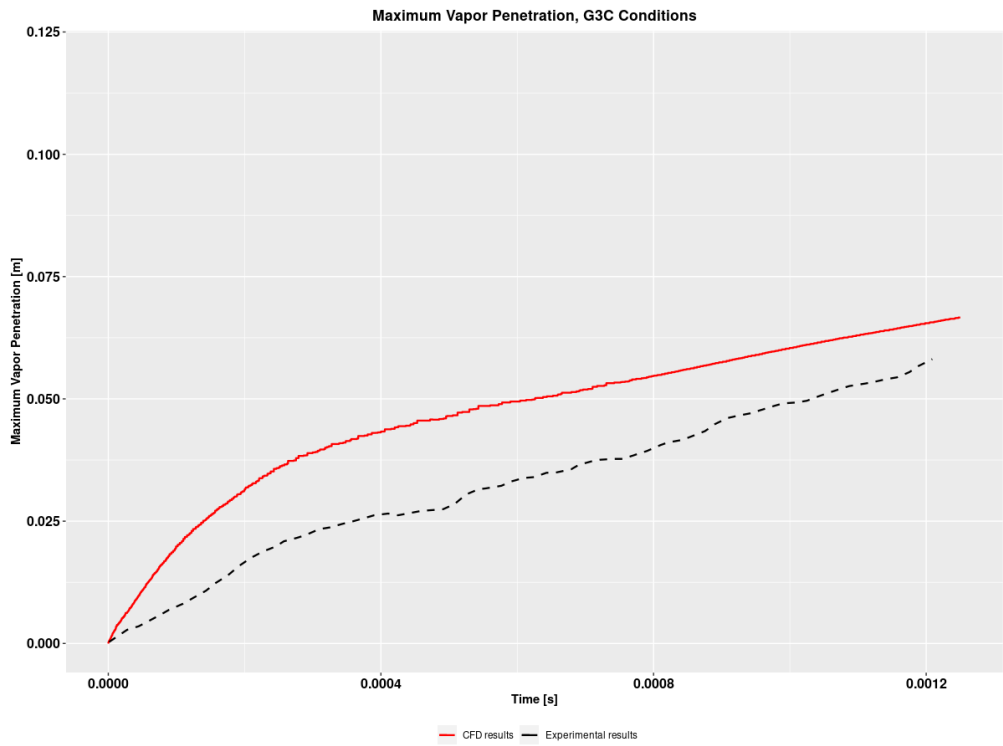


Figure 4.2: Maximum vapor penetration

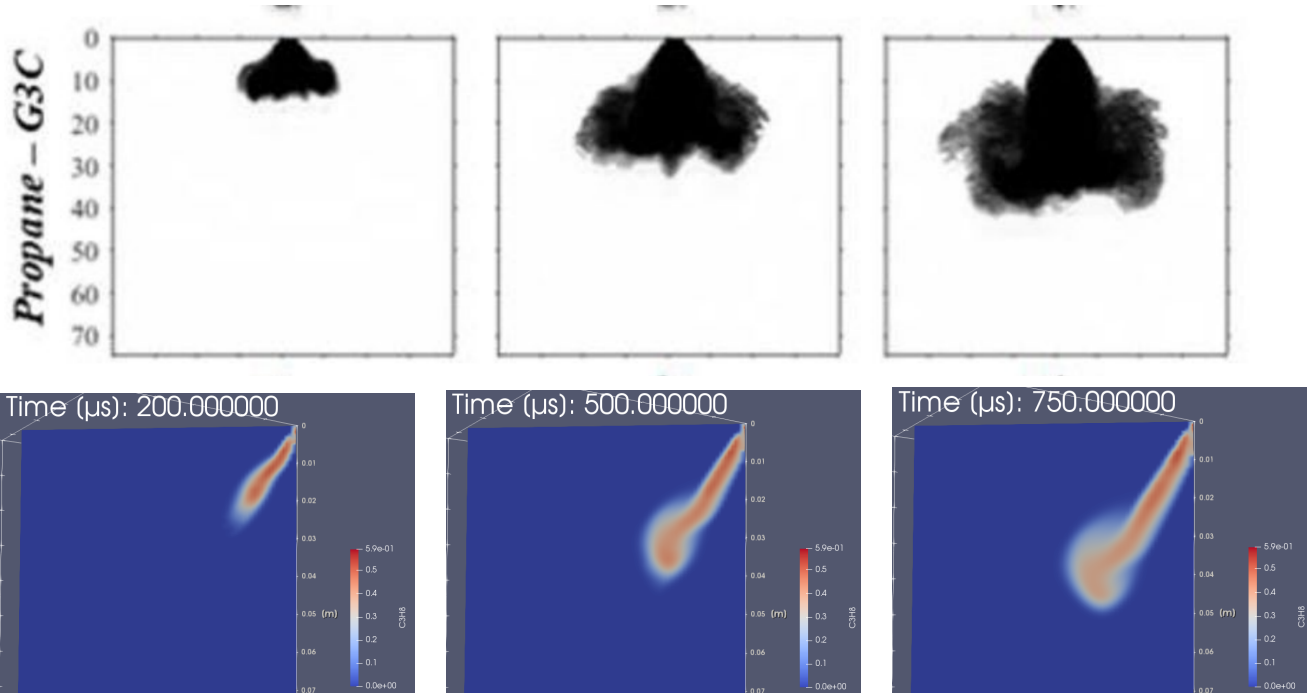


Figure 4.3: Propane concentration at various timesteps denoted after start of injection. High-speed Schlieren images on top from Windell et.al. [18] (penetration scale in *mm*) and CFD-results at corresponding timesteps below

The contour plots in figure 4.3 confirms what we can see in the line plots above. For all timesteps examined it can be seen that the penetration is higher for the CFD simulations compared to the experimental results. The profile of the contour overall correspond somewhat well. However, the simulation results does not show the same width and large size of spray cloud at the later timesteps. In figure 4.4, the particle diameter distribution for the three timesteps can be seen. Here we can see, as expected, that in general the particle diameter increases the further away from the injector it is. When the diameter reaches a large enough value the particles evaporate.

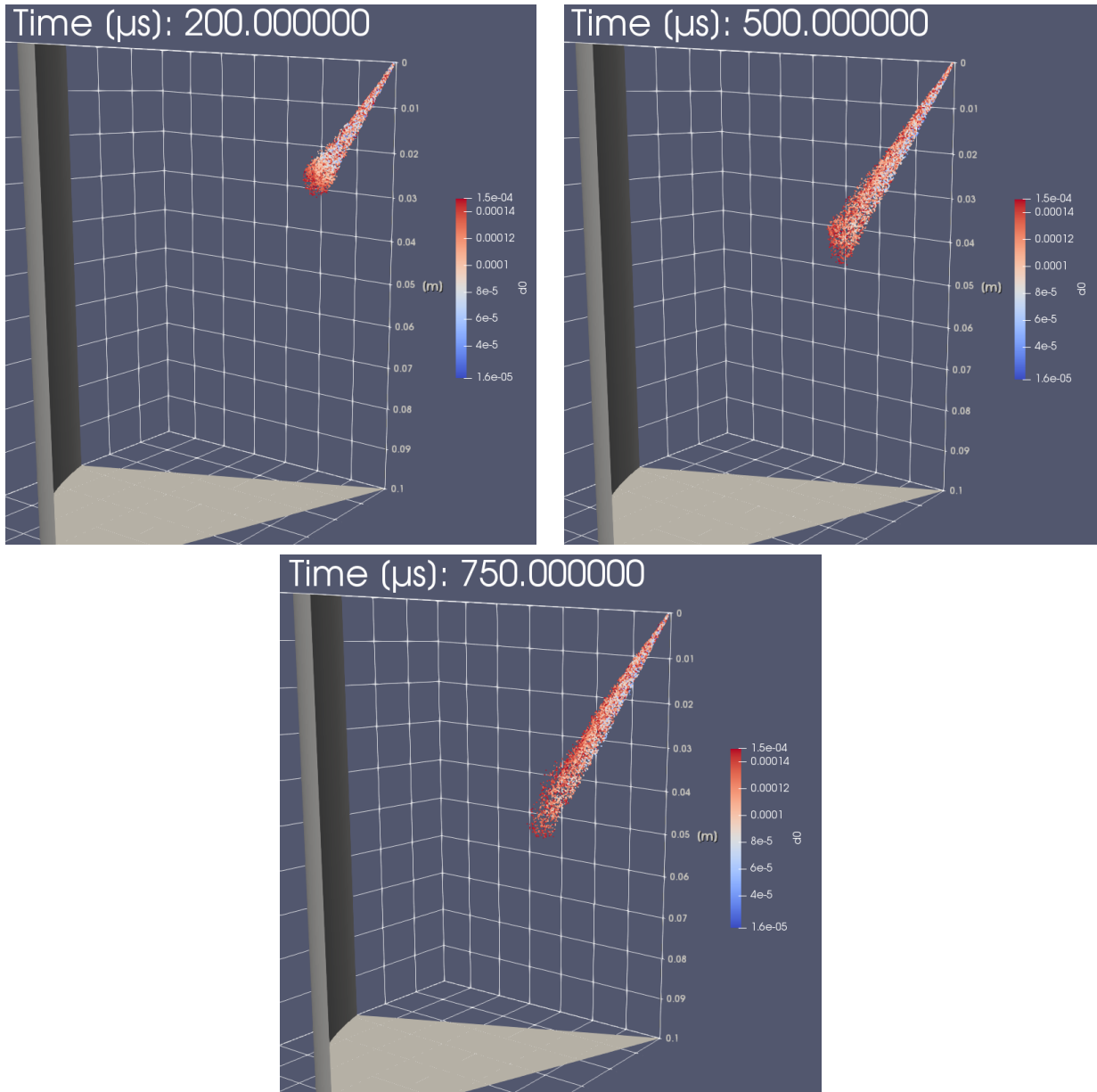


Figure 4.4: Particle diameter distribution in the spray cloud

4.2 Results - Design Of Experiment

4.2.1 2^4 Factorial Design

To examine the results and to see which parameters were significant for the response, the effect of the factors were plotted. Furthermore the parameters were plotted in conjunction with each other to see if there were any interaction between the parameters.

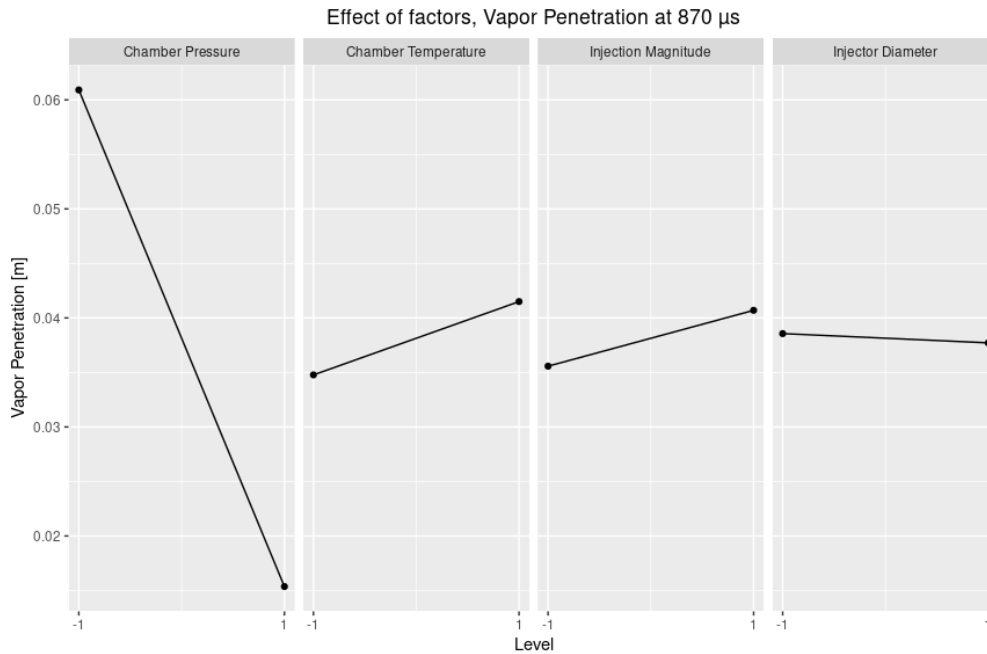


Figure 4.5: Effect of factors for vapor penetration at end of injection

The effect of factors for the vapor penetration and liquid penetration at end of injection can be seen in figure 4.5 and 4.6 respectively. The figures shows that chamber pressure has the largest effect on the response, both when looking at vapor and liquid penetration. For both the responses, the penetration decreases a large amount when the chamber pressure is at the high level of 50 bars.

In general, the results for both penetrations look highly similar for all factors except injection magnitude. Here it can be seen that the vapor penetration slightly increases when increasing the magnitude. However, for the liquid penetration, it can be seen that the penetration decreases when increasing the injection magnitude. It can also be seen that the injection magnitude is more significant for the response when looking at liquid penetration as the gradient of the curve is larger compared to the vapor penetration response.

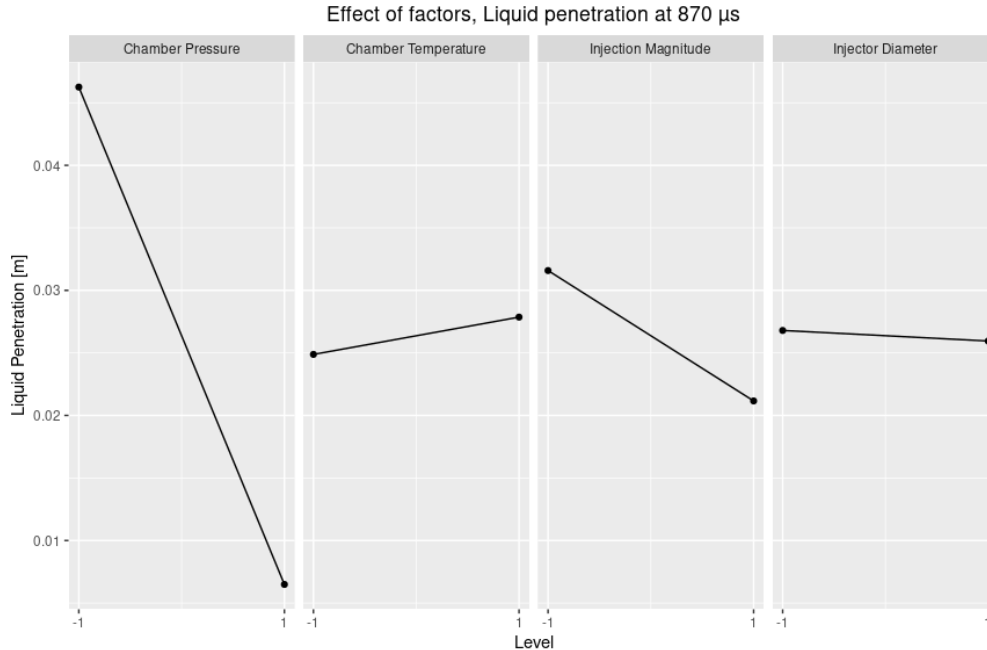


Figure 4.6: Effect of factors for liquid penetration at end of injection

In figure 4.7 and 4.8 the interaction between the factors can be seen for both examined responses. The plots can be interpreted such that, the less parallel the lines for each factor is, the more they interact with each other. For the liquid penetration in figure 4.7 it can be seen that there is a clear interaction between chamber pressure and chamber temperature where the two lines crosses each other when reaching the high level in chamber pressure. It can also be seen that the chamber pressure and injection magnitude interact with each other, giving bigger decrease in penetration length at a low injection magnitude compared to a high one when the chamber pressure is at a high level. For the other factors the interaction is very small and not as significant as for the ones stated above, however none of the lines are completely parallel meaning there is some interaction between all factors when examining liquid penetration.

For the vapor penetration, figure 4.8, there is not a large interaction between the majority of the factors. For this response, the largest interaction is between the injection magnitude and chamber temperature. When the chamber temperature is at a high level, the vapor penetration increases a larger amount at a high injection magnitude, compared to when the chamber temperature is at the low value. Furthermore, some interaction can be seen between injector diameter and injection magnitude. In general however, the lines in the interaction plots are to a greater extent parallel with each other compared to the interactions for the liquid penetration response. This means, according to the model, that less interaction is occurring between the factors when analysing vapor penetration at end of injection compared to liquid penetration.

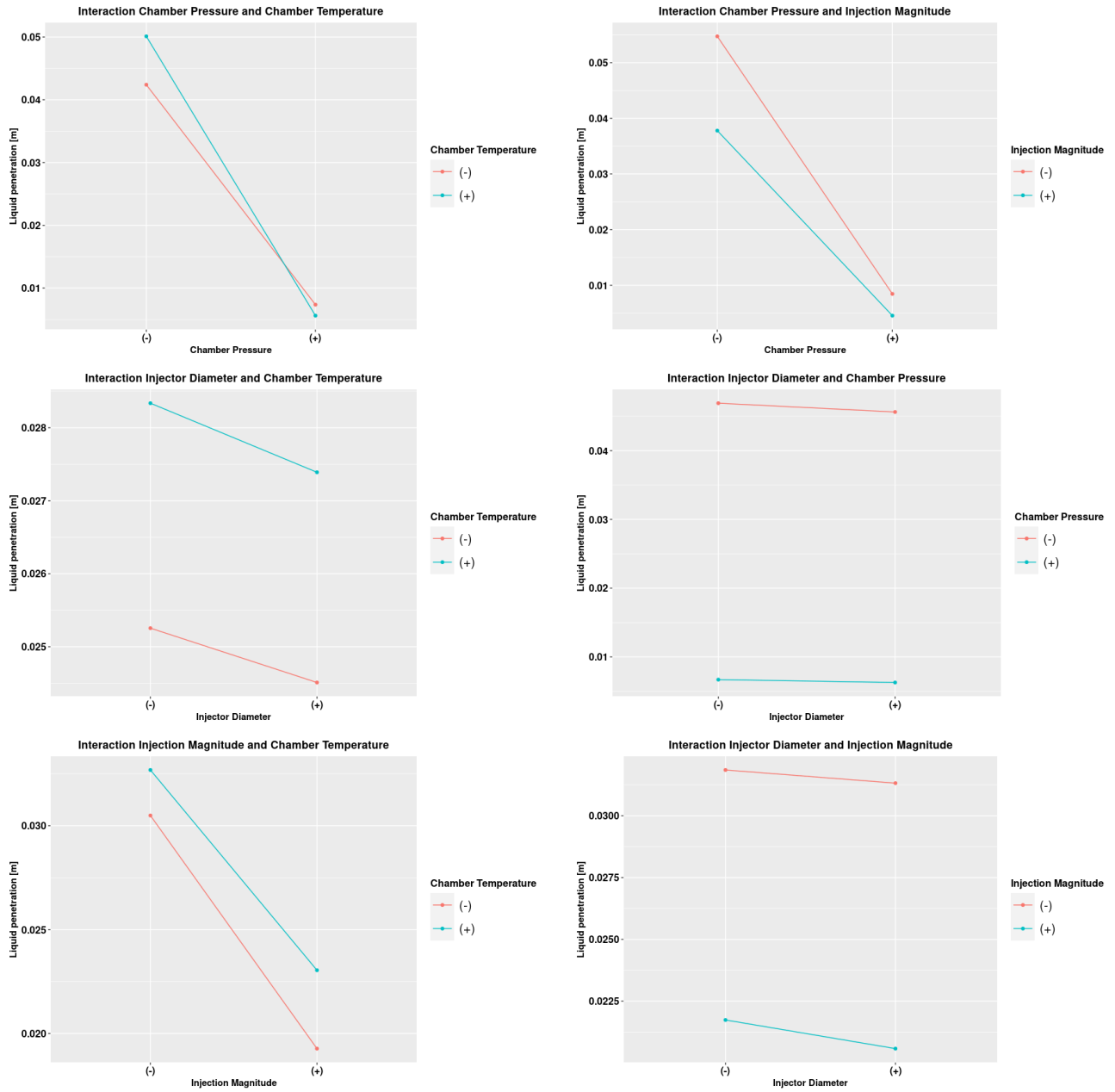


Figure 4.7: Interaction between factors looking at liquid penetration at end of injection

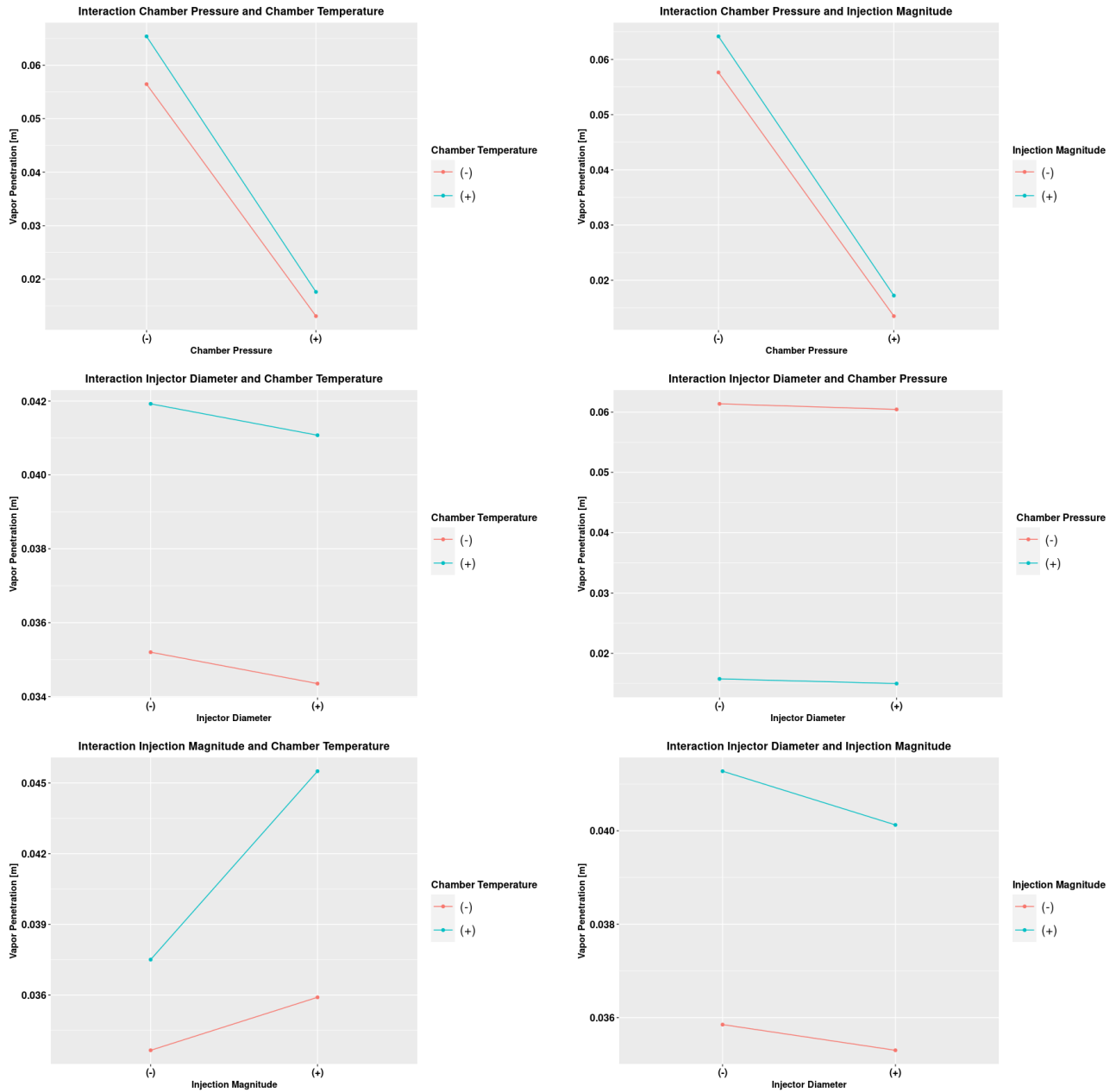


Figure 4.8: Interaction between factors looking at vapor penetration at end of injection

The results for the ANOVA tests are shown in figure 4.9. The analysis resulted in that all four factors have some significance for both vapor and liquid penetration as a response. What can be seen however is that chamber pressure has a higher significance than the others, this is shown by the p-value being quite a bit smaller than for the other factors. Furthermore, the results show that the chamber temperature does not have an as large significance for the liquid penetration as for the vapor penetration. The numbers also show us that the interaction between injection magnitude and chamber pressure, injection magnitude and chamber temperature and also the interaction between chamber pressure and chamber temperature are significant for both of the examined responses.

All of the results from the ANOVA tests correspond well to what can be observed in the effect of factors and interaction plots presented above in figures 4.5, 4.6, 4.7 and 4.8.


```

Df    Sum Sq  Mean Sq  F value  Pr(>F)
Injector_D      1 0.000003 0.000003 1.284e+02 0.05603 .
Injection_U      1 0.000105 0.000105 4.669e+03 0.00932 **
Chamber_P       1 0.008299 0.008299 3.689e+05 0.00105 **
Chamber_T       1 0.000181 0.000181 8.040e+03 0.00710 **
Injector_D:Injection_U      1 0.000000 0.000000 1.600e+01 0.15596
Injector_D:Chamber_P      1 0.000000 0.000000 1.000e+00 0.50000
Injector_D:Chamber_T      1 0.000000 0.000000 0.000e+00 1.00000
Injection_U:Chamber_P      1 0.000008 0.000008 3.484e+02 0.03407 *
Injection_U:Chamber_T      1 0.000033 0.000033 1.469e+03 0.01660 *
Chamber_P:Chamber_T      1 0.000019 0.000019 8.604e+02 0.02169 *
Injector_D:Injection_U:Chamber_P      1 0.000000 0.000000 1.110e-01 0.79517
Injection_U:Chamber_P:Chamber_T      1 0.000000 0.000000 2.178e+01 0.13439
Injector_D:Chamber_P:Chamber_T      1 0.000000 0.000000 1.110e-01 0.79517
Injector_D:Injection_U:Chamber_T      1 0.000000 0.000000 4.440e-01 0.62567
Residuals      1 0.000000 0.000000
---
Signif. codes:  0 '***' 0.001 '**' 0.01 '*' 0.05 '.' 0.1 ' ' 1
>

```

(a) Vapor Penetration

```

Df    Sum Sq  Mean Sq  F value  Pr(>F)
Injector_D      1 0.000003 0.000003 6.729e+01 0.07722 .
Injection_U      1 0.000435 0.000435 1.023e+04 0.00629 **
Chamber_P       1 0.006326 0.006326 1.489e+05 0.00165 **
Chamber_T       1 0.000036 0.000036 8.365e+02 0.02200 *
Injector_D:Injection_U      1 0.000000 0.000000 9.236e+00 0.20237
Injector_D:Chamber_P      1 0.000001 0.000001 1.741e+01 0.14975
Injector_D:Chamber_T      1 0.000000 0.000000 9.580e-01 0.50680
Injection_U:Chamber_P      1 0.000170 0.000170 4.001e+03 0.01006 *
Injection_U:Chamber_T      1 0.000003 0.000003 5.892e+01 0.08247 .
Chamber_P:Chamber_T      1 0.000089 0.000089 2.105e+03 0.01387 *
Injector_D:Injection_U:Chamber_P      1 0.000000 0.000000 1.129e+01 0.18416
Injection_U:Chamber_P:Chamber_T      1 0.000000 0.000000 4.608e+00 0.27755
Injector_D:Chamber_P:Chamber_T      1 0.000000 0.000000 3.620e-01 0.65518
Injector_D:Injection_U:Chamber_T      1 0.000000 0.000000 5.300e-02 0.85616
Residuals      1 0.000000 0.000000
---
Signif. codes:  0 '***' 0.001 '**' 0.01 '*' 0.05 '.' 0.1 ' ' 1
> |

```

(b) Liquid Penetration

Figure 4.9: Results ANOVA test from 2^4 factorial design for, (a) Vapor penetration (b) Liquid penetration

4.2.2 Latin Hypercube Design

The ANOVA tests for the Latin hypercube design shows that we have low p-values, thus significance, for injection magnitude and chamber pressure when looking at the vapor penetration. Furthermore, the analysis show significance when interaction between injection magnitude and chamber pressure occurs. One thing to note for both vapor and liquid penetration is that the test shows that significance is noteworthy when three factors interact. One example is in the liquid penetration where the results show quite a large significance when injector diameter, injection magnitude and chamber pressure interact. For the liquid penetration there are three instances where three factors interacting shows significance, for the vapor penetration there is one instance present.

For the liquid penetration the ANOVA tests show a larger amount of factors being significant for the response compared to the vapor penetration. For this response, all factors have some significance with chamber pressure being the most significant. According to the test, almost all combination of factors have some significance

for the response, something that is not present for the vapor penetration response.

	Df	Sum Sq	Mean Sq	F value	Pr(>F)
Injector.D	1	0.0000090	0.0000090	15.411	0.1588
Injection.U	1	0.0003560	0.0003560	606.746	0.0258 *
Chamber.P	1	0.0012030	0.0012030	2050.093	0.0141 *
Chamber.T	1	0.0000192	0.0000192	32.657	0.1103
Injector.D:Injection.U	1	0.0000127	0.0000127	21.681	0.1347
Injector.D:Chamber.P	1	0.0000091	0.0000091	15.466	0.1585
Injector.D:Chamber.T	1	0.0000014	0.0000014	2.459	0.3614
Injection.U:Chamber.P	1	0.0002233	0.0002233	380.590	0.0326 *
Injection.U:Chamber.T	1	0.0000932	0.0000932	158.808	0.0504 .
Chamber.P:Chamber.T	1	0.0000083	0.0000083	14.181	0.1652
Injector.D:Injection.U:Chamber.P	1	0.0000976	0.0000976	166.345	0.0493 *
Injection.U:Chamber.P:Chamber.T	1	0.0000088	0.0000088	15.030	0.1607
Injector.D:Chamber.P:Chamber.T	1	0.0000146	0.0000146	24.864	0.1260
Injector.D:Injection.U:Chamber.T	1	0.0000000	0.0000000	0.006	0.9515
Residuals	1	0.0000006	0.0000006		

 Signif. codes: 0 '***' 0.001 '**' 0.01 '*' 0.05 '.' 0.1 ' ' 1
 > |

(a) Vapor Penetration

	Df	Sum Sq	Mean Sq	F value	Pr(>F)
Injector.Diameter	1	0.0000159	0.0000159	223.809	0.04249 *
Injection.Magnitude	1	0.0000233	0.0000233	328.135	0.03511 *
Chamber.Pressure	1	0.0003829	0.0003829	5381.066	0.00868 **
Chamber.Temperature	1	0.0000048	0.0000048	66.941	0.07743 .
Injector.Diameter:Injection.Magnitude	1	0.0000079	0.0000079	110.501	0.06038 .
Injector.Diameter:Chamber.Pressure	1	0.0000296	0.0000296	416.396	0.03117 *
Injector.Diameter:Chamber.Temperature	1	0.0000006	0.0000006	7.874	0.21794
Injection.Magnitude:Chamber.Pressure	1	0.0002559	0.0002559	3596.681	0.01061 *
Injection.Magnitude:Chamber.Temperature	1	0.0002574	0.0002574	3617.485	0.01058 *
Chamber.Pressure:Chamber.Temperature	1	0.0000012	0.0000012	16.823	0.15224
Injector.Diameter:Injection.Magnitude:Chamber.Pressure	1	0.0002062	0.0002062	2898.306	0.01182 *
Injection.Magnitude:Chamber.Pressure:Chamber.Temperature	1	0.0000195	0.0000195	273.964	0.03842 *
Injector.Diameter:Chamber.Pressure:Chamber.Temperature	1	0.0000177	0.0000177	248.461	0.04033 *
Injector.Diameter:Injection.Magnitude:Chamber.Temperature	1	0.0000001	0.0000001	1.281	0.46072
Residuals	1	0.0000001	0.0000001		

 Signif. codes: 0 '***' 0.001 '**' 0.01 '*' 0.05 '.' 0.1 ' ' 1
 > |

(b) Liquid Penetration

Figure 4.10: Results ANOVA test from Latin Hypercube design for, (a) Vapor penetration (b) Liquid penetration

The contour plots for the examined responses, figure 4.11 and 4.12, give some indication on how the parameters interact with each other. A common denominator for both responses is the position of the highest point for each parameter interaction. For all plots it is visible that the highest point is located at roughly the same position. The contour plots give an indication on the parameter values and how they affect the response variable. It is for example possible to see that when the chamber pressure is low and the injection magnitude is high, the vapor and liquid penetration will be at its highest point. One thing to note however is that it is not possible to see the values of the two other parameters present in the simulation. As the Latin hypercube design chooses random values for all parameters it is difficult to get a clear understanding how all four parameters affect the response from the contour plots.

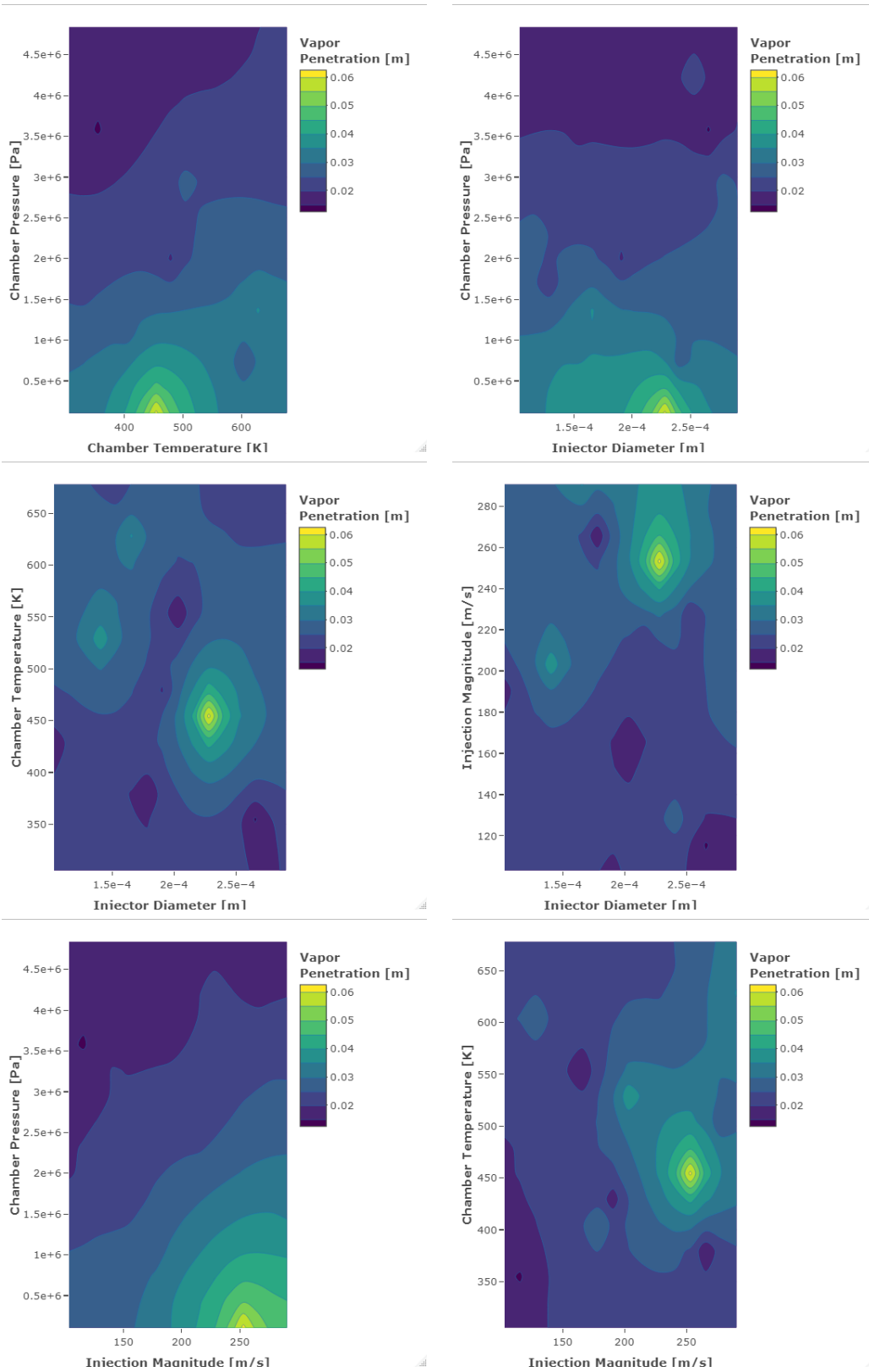


Figure 4.11: Contour plots showing interaction between parameters for vapor penetration at end of injection

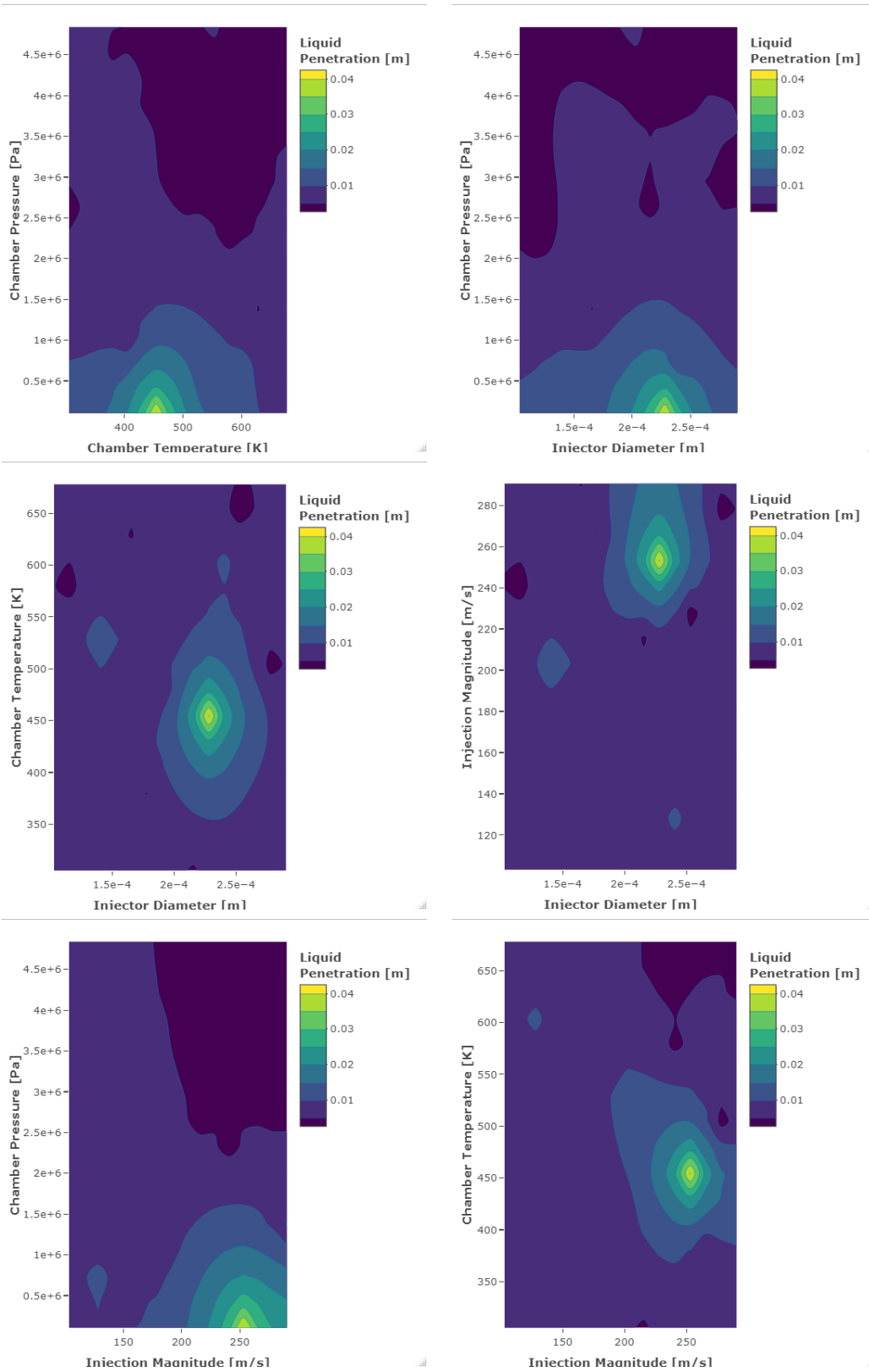


Figure 4.12: Contour plots showing interaction between parameters for liquid penetration at end of injection

Chapter 5

Discussion

5.1 CFD Section

When comparing the simulated results with the experiment from Windell et.al. [18] it can be seen that the results correlate to some degree. For the liquid penetration, roughly the same maximum value is obtained at the same timestep. However, the profile of the curve does not correlate well, with the experiment having a more smooth profile with a constant increase of penetration length while the simulations show a large penetration in the beginning with a plateau at 875 μs to then increase again.

For the liquid penetration, the profile of the experiment and simulation correlate fairly good having a steady and smooth increase in penetration. However, the simulations have a translation upwards resulting in a constant higher penetration length compared to the experimental results.

The reason for the non correlating results has most likely to do with the injection profile of the fuel. As the mass injected in the experiments was not specified, the injection profile was assumed to be a constant velocity during the injection duration. The behaviour of the liquid penetration with a plateau and a increase in the last quarter of the examined time is also most probable due to the injection profile. To get more accurate simulated results, the injection profile should be tweaked and further worked with. However, for the purpose of this thesis and due to time constraints, it was decided that the results obtained were sufficient for the DoE implementation.

5.2 Design Of Experiment Section

The results from the factorial design concluded that the chamber pressure had a large effect on both responses examined. The reason for this large significance could be that the difference between the high and low value for the factor is large. When looking at the other factors, the relative difference between the high and low values are a lot lower. Furthermore, when conducting a regular full factorial design of experiment, every response is assumed to follow a linear function. If the response for a particular factor does not follow a linear function this will not be picked up by the design. To resolve this issue, one solution could be to add center points between the high and low value for all factors. With the help of an extra point in the domain the response could be modeled with a curvature if necessary.

Something to note when analysing the results from the factorial design of experiment is that the model is not made for deterministic responses, a type response that occurs when conducting computer experiments. The model needs replicates to be able to calculate an aggregate response. With this aggregated response the model can then calculate mean differences and variations in the response. The deterministic nature of the response in this thesis may affect the results in the factorial model, something that has to be taken into consideration when analysing the results.

The Latin hypercube design is, unlike the factorial design, created for experiments with deterministic responses. This means that the model is more suitable for usage when conducting computer experiment such as CFD simulations. However, as the design spreads out the point randomly in the design domain, it is more difficult to analyse significance and interaction between factors in such a systematic order that is possible for the factorial design. The contour plots give an overview of how different factors affect the response, however seeing interactions between all variables is somewhat difficult and not as easy as for the line plots created for the factorial design. As there is not, to the authors knowledge, any way of directly comparing the interactions and significance of factors between the two models except for ANOVA tests, direct comparison of the two models is difficult.

The ANOVA tests for the two different designs gave an indication on which factor and which interactions between the factors that are significant for the examined responses. The factorial design gave a smaller amount of significant factors and significant interactions but it gave a higher level of significance for the ones pointed out by the ANOVA test. The high F-values and thus low p-values from the factorial design makes the significance test more trustworthy compared to the ANOVA tests conducted on the Latin hypercube design. Furthermore, the tests conducted on the Latin hypercube design showed significant interaction between three factors, something that seems unreasonable from a physical standpoint. The chance of three factors interacting and affecting the response significantly is low and as the ANOVA tests for the factorial design does not show the same three way interaction, this interaction can be questioned. To note however is that three way interaction is not unfeasible and that the results from the ANOVA test for the Latin hypercube design should not be completely overlooked.

The results from the simulations and the factorial design showing significant parameters and interaction between parameters are reasonable and follow what is physically expected. The results show for example that with lower ambient pressure, the vapor penetration will increase and with higher ambient temperature the vapor penetration will increase. These results are reasonable and correlate well with results from experiments conducted by Windell et.al [18], Du et.al [31] and Shervani-Tabar et.al [32]. However, one result that does not correlate between experiments and the simulated results has to do with liquid penetration and injection magnitude or pressure. In the experimental results the liquid penetration increases with higher injection pressures. The results from the simulations and factorial DoE however shows that the liquid penetration decreases with an increase in injection magnitude. There are many parameters that could affect why the response for the liquid penetration is different for the experiments compared to the simulations. One might be the ambient conditions resulting in a higher or lower amount of evaporation of the fuel. Furthermore, the type of fuel affects when and how the evaporation occurs, in the experiments looking at injection pressure Diesel and gasoline are the investigated fuels. The faster the evaporation, the shorter the liquid penetration is. Another thing affecting the evaporation of the droplets in the simulation is the evaporation model, as the parameters for the KHRT model is optimised for gasoline the evaporation behaviour of the injected propane might not be fully correct.

A response variable that would be interesting to examine for the design of experiment part is the mixing of the fuel in the combustion chamber. To achieve good efficiency and correct condition for a good combustion, a certain amount of mixing of the fuel and air is often specified. When looking at this response however, it is important that the same mass of fuel is injected for every examined case as often the mass of the injected fuel is specified to a set number. The mixing should be optimised for the specified mass of fuel injected resulting in a mixing targeted from the start. Changing the injection magnitude, as done for this thesis, while keeping the same injection duration, will result in different masses of fuel being injected. Thus if we want to look at mixing as a response variable for the DoE, the simulation setup needs to be changed ensuring that the same mass of fuel is injected for all cases.

A number of ways of performing analysis was researched during the thesis but due to lack of time no real efforts could be put into applying them. One technique that stood out as particularly interesting was Gaussian process modelling, a process that fits the data and creates a model based on the notion of Gaussian distribution. Some efforts were put into fitting the response data and use the Gaussian process model, however no clear result could be conducted from the data. Results from this can be found in appendix A.

Chapter 6

Conclusions

6.1 Conclusions

The CFD setup constructed for this thesis gives a starting point for injection of LPG using a multi-hole injector. However, due to time constraints an accurate model giving results close to experimental results could not be obtained. To improve the model and results more time should be put into the model. In the set-up, modeling parameters as break-up and flash boiling should be looked into further to increase the accuracy of the model. Furthermore, the injection profile of the fuel should be further worked on. In general the model gave an accurate enough standpoint to perform the DoE analysis with modifiable parameters changing the outcome of the results.

Creating and performing simulations based on two design of experiment types gave an overview of what parameters affected the vapor and liquid penetration of the injected fuel. The models gave similar results showing that injector orifice diameter was the parameter affecting the response the least and chamber pressure the parameter affecting the most of the for examined factors. In general the ANOVA test for the factorial design gave lower p-values and thus a higher confidence that the parameters affected the response. Furthermore the factorial design gave more physical results showing only interaction between two factors, not three as for the Latin hypercube design. Comparing the two models proved difficult and no clear comparison technique between the two models could be found during the work on this thesis. Finding an optimal and quick DoE model requires further work and investigation.

The tools used for the completion of this thesis has mainly been OpenFOAM-8 and Rstudio. Rstudio gives a good GUI for the R programming language and is quite easy and comfortable to use if the user has operated similar programs such as MATLAB. Furthermore, Rstudio is an open source program with a large amount of users making it easy to find guides and information online. As the R programming language is created for statistical computing it is very suitable for performing design of experiments and other statistical tasks such as ANOVA tests. There is a large number of packages created by users online that can be downloaded and used for free in Rstudio. The packages are an excellent tool giving the user an easy way of doing tasks such as designing a Latin hypercube design and much more. The packages reduce the amount of code the user has to write and makes designing and analysing quick and easy. Furthermore, a large amount of the packages has documentation describing how the specific package can be used. Rstudio also contains a large number of plotting tools and packages making it possible to create attractive and clear looking plots and figures, an important aspect to present understandable and clear results. From the work made in Rstudio for this thesis it can be concluded that the program is a good and powerful tool for creating and evaluating design of experiments and presenting the obtained results. More work in the program can give powerful and easy to manage automation scripts both conducting statistical analysis and presenting the results instantly.

6.2 Suggestion for future work

To get a more in depth analysis on how to design and optimise both the CFD-model and Design of Experiment models, the work of this thesis could be split in to two different parts.

One part, or study, could have focus on the CFD-modeling and how it could be tweaked to correlate well with the experimental results. Furthermore, this model could be larger than the current one created giving more parameters to change for the DoE part. A suggestion is to make a case consisting of the full combustion chamber, i.e. putting together 8 "slices" that were examined in this thesis constructing a full combustion chamber. This would give more opportunity to change parameters such as injection angle and more. Furthermore, the model could be tweaked in such a way that the same mass of fuel is always injected, this would give opportunity to look at important responses such as mixing.

The second part, or study, could have focus on just developing and optimising the DoE model. For this report a finished, validated CFD-model should be provided together with a number of given responses that should be examined. This would give a greater opportunity to optimise and find the correct model for the DoE, furthermore it would give sufficient time to find good ways of comparing data and models. In this part, Gaussian process modelling and other evaluation models could be analysed in detail.

Bibliography

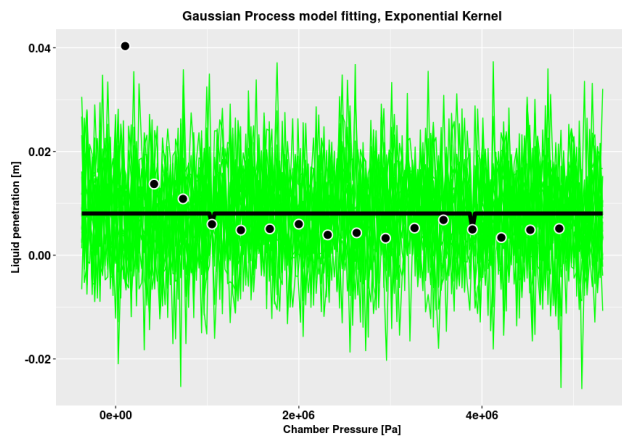
- [1] N. Anner, “How dual-fuel conversions for two- and four-stroke engines prepare vessels to run on green methanol and ammonia,” Accessed: 2023-05-08. [Online]. Available: https://www.man-es.com/discover/potential-dual-fuel-conversions?gad=1&gclid=CjOKCQjwmN2iBhCrARIsAG_G2i6QHbJ1YaDfX0vr dxMpRy3nN3GompePexddBDQ1SJ0FnxHtL1UbNDYaAmzuEALw_wcB.
- [2] K. M. Bower, “What is Design of Experiments (DOE)?,” Accessed: 2023-04-24. [Online]. Available: <https://asq.org/quality-resources/design-of-experiments>.
- [3] OpenCFD Ltd, “About OpenFOAM,” Accessed: 2023-04-12. [Online]. Available: <https://www.openfoam.com/>.
- [4] CFD Online, “Favre averaged Navier-Stokes equations,” Accessed: 2023-04-24. [Online]. Available: https://www.cfd-online.com/Wiki/Favre_averaged_Navier-Stokes_equations.
- [5] M. Vångö, “Cfd modelling of direct gas injection using a lagrangian particle tracking approach,” Jun. 2015. [Online]. Available: <https://lup.lub.lu.se/luur/download?func=downloadFile&recordId=5474127&fileId=7364064>.
- [6] N. Nordin, “Complex chemistry modeling of diesel spray combustion,” 2001, Chalmers University of Technology.
- [7] H. K. Versteeg and W. Malalasekera, *An Introduction to Computational Fluid Dynamics*. 2007, ISBN: 978-0-13-127498-3.
- [8] ANSYS, “ANSYS CFX-solver theory guide. ANSYS CFX release 14.0,” Nov. 2011.
- [9] J. Andric, “CFD with OpenFOAM software, Lagrangian particle tracking,” 2009. [Online]. Available: http://www.tfd.chalmers.se/~hani/kurser/0S_CFD_2009/JelenaAndric/reportJelenaAndric.pdf.
- [10] S. B. Pope, *Turbulent Flows*. Aug. 2000, pp. 373–383, ISBN: 9780521598866.
- [11] X. Wang and H. Zhao, “Numerical simulation of the gasoline spray with an outward-opening piezo-electric injector: A comparative study of different breakup models,” Apr. 2018, SAE Technical Paper 2018-01-0272. DOI: <https://doi.org/10.4271/2018-01-0272>.
- [12] M. H. H. Ishak, F. Ismail, S. C. Mat, M. S. A. Aziz, M. Z. Abdullah, and A. Abas, “Numerical study on the influence of nozzle spray shape on spray characteristics using diesel and biofuel blends,” *Biofuels*, vol. 12, no. 9, pp. 1109–1121, 2021. DOI: 10.1080/17597269.2019.1583717.
- [13] M. Alderliesten, “Mean particle diameters. part vii. the rosin-rammler size distribution: Physical and mathematical properties and relationships to moment-ratio defined mean particle diameters,” *Particle & Particle Systems Characterization*, vol. 30, no. 3, pp. 244–257, 2013. DOI: <https://doi.org/10.1002/ppsc.201200021>. eprint: <https://onlinelibrary.wiley.com/doi/pdf/10.1002/ppsc.201200021>. [Online]. Available: <https://onlinelibrary.wiley.com/doi/abs/10.1002/ppsc.201200021>.
- [14] OpenFOAM: API Guide v2112, “RosinRammler, Detailed Description,” Accessed: 2023-04-18. [Online]. Available: https://www.openfoam.com/documentation/guides/latest/api/classFoam_1_1distributionModels_1_1RosinRammler.html.

- [15] European Commission, European Alternative Fuels Observatory, “Alternative fuels,” Accessed: 2023-04-25. [Online]. Available: <https://alternative-fuels-observatory.ec.europa.eu/general-information/alternative-fuels>.
- [16] U.S. Department of Energy, “Propane fuel basics,” Accessed: 2023-04-05. [Online]. Available: https://afdc.energy.gov/fuels/propane_basics.html.
- [17] U.S. Department of Energy, “Fuel properties comparison,” Accessed: 2023-04-05. [Online]. Available: <https://afdc.energy.gov/fuels/properties>.
- [18] B. Windell, M. Sharma, L. Nocivelli, K. Asztalos, *et al.*, “Bulk spray and individual plume characterization of LPG and iso-octane sprays at engine-like conditions,” Jan. 2022, SAE Technical Paper 2022-01-0497. DOI: 10.4271/2022-01-0497.
- [19] M. Mojtabi, N. Chadwick, G. Wigley, and J. Helie, “The effect of flash boiling on break up and atomization in GDI sprays,” 2008. [Online]. Available: https://ilasseurope.org/ICLASS/ILASS2008_COMO/file/papers/6-1.pdf.
- [20] S. Suma and M. Koizumi, “Internal boiling atomization by rapid pressure reduction of liquids,” *Trans JSME (B)*, vol. 43, pp. 4608–4617, 1977.
- [21] D. Kawano, H. Ishii, H. Suzuki, Y. Goto, M. Odaka, and J. Senda, *Numerical study on flash-boiling spray of multicomponent fuel*. Jun. 2006, pp. 309–385. DOI: <https://doi.org/10.1002/htj.20117>.
- [22] D. C. Montgomery, *Design and analysis of experiments - 8th edition*. Apr. 2012, ISBN: 978-1118146927.
- [23] D. Selvamuthu and D. Das, *Multifactor Experimental Designs*. 2018, ISBN: 978-981-13-1736-1.
- [24] J. Borkowski, “Response surface methodology, STAT 578,” 2014. [Online]. Available: <https://www.math.montana.edu/jobost578/sec4a.pdf>.
- [25] C. Natoli and S. Burke, “Computer experiments: Space filling design and gaussian process modeling,” Mar. 2018. [Online]. Available: https://www.afil.edu/stat/statcoe_files/Computer%20Experiments-%20Space%20Filling%20Designs%20and%20Gaussian%20Process%20Modeling.pdf.
- [26] R. Bevans, “One-way ANOVA — When and How to Use It (With Examples),” Mar. 2020, Accessed: 2023-04-29. [Online]. Available: <https://www.scribbr.com/statistics/one-way-anova/>.
- [27] Engine Combustion Network, ““Spray G” operating conditions,” Accessed: 2023-04-13. [Online]. Available: <https://ecn.sandia.gov/gasoline-spray-combustion/target-condition/spray-g-operating-condition/>.
- [28] E. L. Cano, J. M. Moguerza, M. Prieto, *et al.* “Sixsigma: Six sigma tools for quality control and improvement.” Accessed: 2023-04-09. (Apr. 2023), [Online]. Available: <https://CRAN.R-project.org/package=SixSigma>.
- [29] S. Ba and V. R. Joseph. “Maxpro: Maximum projection designs.” Accessed: 2023-03-14. (Sep. 2018), [Online]. Available: <https://CRAN.R-project.org/package=MaxPro>.
- [30] Engine Combustion Network, ““Spray G” specified nozzle geometry,” Accessed: 2023-04-13. [Online]. Available: <https://ecn.sandia.gov/gasoline-spray-combustion/computational-method/mesh-and-geometry/>.
- [31] J. Du, B. Mohan, J. Sim, T. Fang, and W. L. Roberts, “Experimental and analytical study on liquid and vapor penetration of high-reactivity gasoline using a high-pressure gasoline multi-hole injector,” *Applied Thermal Engineering*, vol. 163, pp. 114–187, 2019, ISSN: 1359-4311. DOI: <https://doi.org/10.1016/j.applthermaleng.2019.114187>.
- [32] M. T. Shervani-Tabar, M. Sheykhvazayefi, and M. Ghorbani, “Numerical study on the effect of the injection pressure on spray penetration length,” *Applied Mathematical Modelling*, vol. 37, no. 14, pp. 7778–7788, 2013, ISSN: 0307-904X. DOI: <https://doi.org/10.1016/j.apm.2013.03.002>. [Online]. Available: <https://www.sciencedirect.com/science/article/pii/S0307904X13001571>.

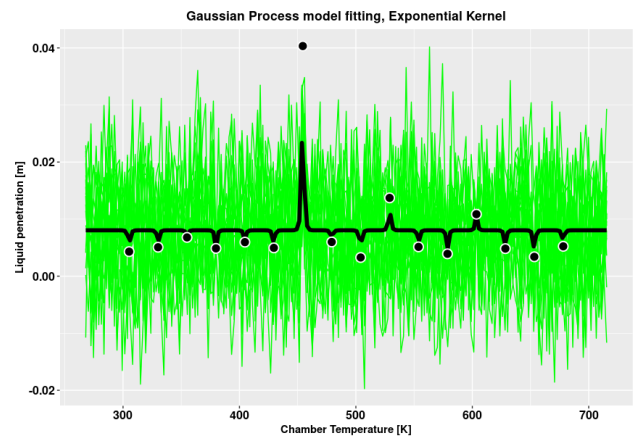
Appendix A

Plots Gaussian Process Modelling

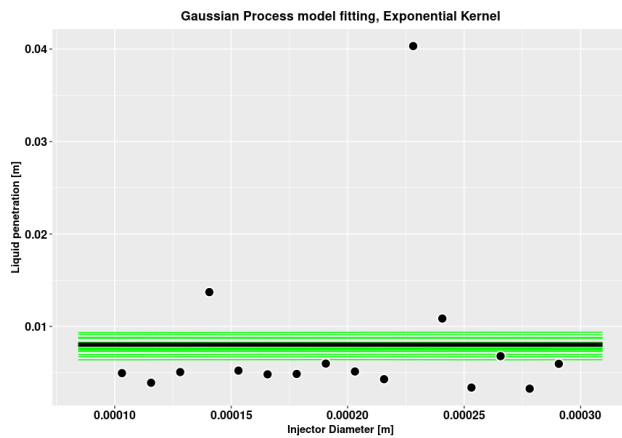
A.1 Liquid Penetration



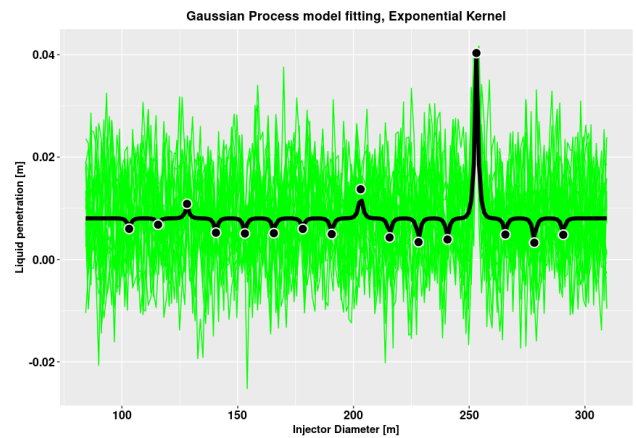
(a) Chamber Pressure



(b) Chamber Temperature



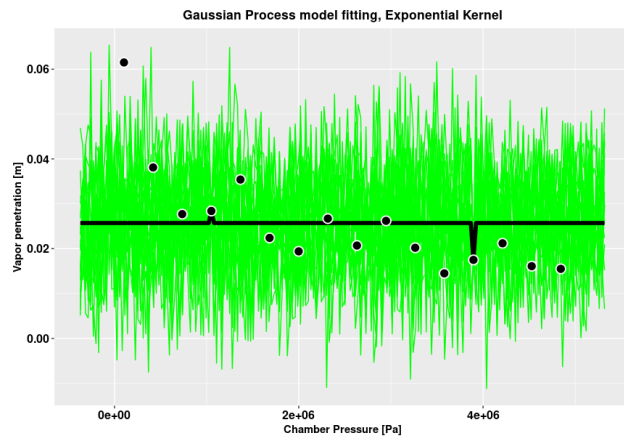
(c) Injector Diameter



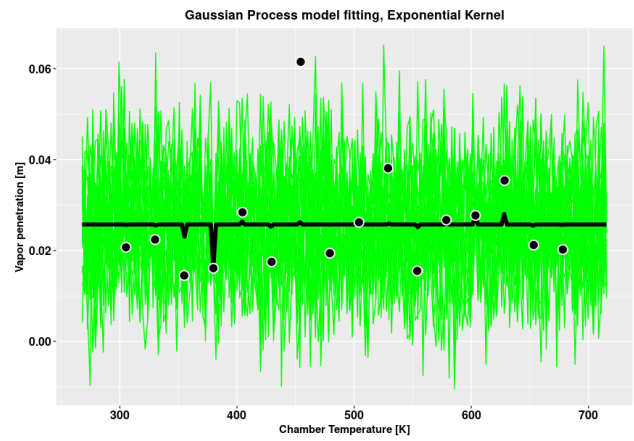
(d) Injection Magnitude

Figure A.1: Model fitting using Gaussian process with an Exponential kernel, Liquid penetration

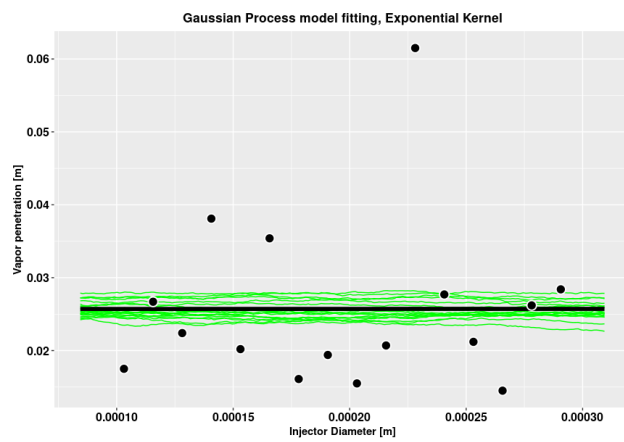
A.2 Vapor Penetration



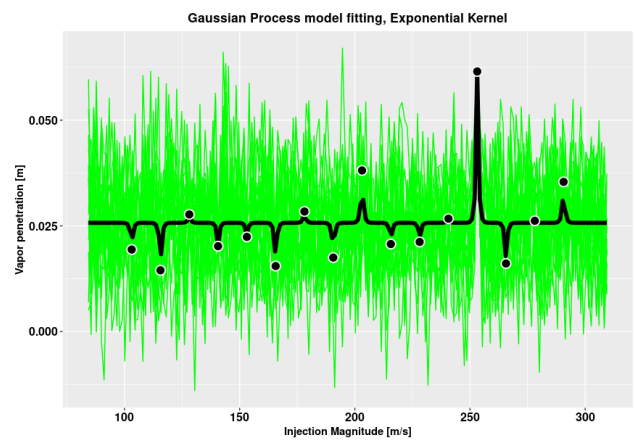
(a) Chamber Pressure



(b) Chamber Temperature



(c) Injector Diameter



(d) Injection Magnitude

Figure A.2: Model fitting using Gaussian process with an Exponential kernel, Vapor penetration

Appendix B

R code

B.1 Contour Plots Lattice Hypercube Design

```
1
2
3
4 library(plotly)
5 library(ggplot2)
6
7
8 injection.data <- read.csv("C:/Users/knase/Desktop/Master ...
   Thesis/CSV_files/Lattice-hyper-liq-pen.870.csv", header = TRUE)
9
10
11
12
13 IDCT <- plot_ly(x=injection.data$Injector.Diameter, y=injection.data$Chamber.Temperature, ...
   z=injection.data$Liquid.Penetration, type = "contour") %>%
14   layout(xaxis= list(title = "<b>Injector Diameter [m]</b>", showexponent = "all", ...
   exponentformat = "e"), yaxis= list(title = "<b>Chamber Temperature [K]</b>")) %>%
15   colorbar(title="<b>Liquid \nPenetration [m]</b>")
16
17 IDCT
18
19
20 IDIM <- plot_ly(x=injection.data$Injector.Diameter, y=injection.data$Injector.Magnitude, ...
   z=injection.data$Liquid.Penetration, type = "contour") %>%
21   layout(xaxis= list(title = "<b>Injector Diameter [m]</b>", showexponent = "all", ...
   exponentformat = "e"), yaxis= list(title = "<b>Injection Magnitude [m/s]</b>")) %>%
22   colorbar(title="<b>Liquid \nPenetration [m]</b>")
23
24 IDIM
25
26 IDCP <- plot_ly(x=injection.data$Injector.Diameter, y=injection.data$Chamber.Pressure, ...
   z=injection.data$Liquid.Penetration, type = "contour") %>%
27   layout(xaxis= list(title = "<b>Injector Diameter [m]</b>", showexponent = "all", ...
   exponentformat = "e"), yaxis= list(title = "<b>Chamber Pressure [Pa]</b>", ...
   showexponent = "all", exponentformat = "e")) %>%
28   colorbar(title="<b>Liquid \nPenetration [m]</b>")
29
30 IDCP
31
32 IMCP <- plot_ly(x=injection.data$Injector.Magnitude, y=injection.data$Chamber.Pressure, ...
   z=injection.data$Liquid.Penetration, type = "contour") %>%
33   layout(xaxis= list(title = "<b>Injection Magnitude [m/s]</b>"), yaxis= list(title = ...
   "<b>Chamber Pressure [Pa]</b>", showexponent = "all", exponentformat = "e")) %>%
34   colorbar(title="<b>Liquid \nPenetration [m]</b>")
35
```

```

36 IMCP
37
38 IMCT <- plot_ly(x=injection.data$Injection.Magnitude, ...
  y=injection.data$Chamber.Temperature, z=injection.data$Liquid.Penetration, type = ...
  "contour") %>%
39 layout(xaxis= list(title = "<b>Injection Magnitude [m/s]</b>"), yaxis= list(title = ...
  "<b>Chamber Temperature [K]</b>")) %>%
40 colorbar(title="<b>Liquid \nPenetration [m]</b>")
41
42 IMCT
43
44 CTCP <- plot_ly(x=injection.data$Chamber.Temperature, y=injection.data$Chamber.Pressure, ...
  z=injection.data$Liquid.Penetration, type = "contour") %>%
45 layout(xaxis= list(title = "<b>Chamber Temperature [K]</b>"), yaxis= list(title = ...
  "<b>Chamber Pressure [Pa]</b>",showexponent = "all", exponentformat = "e")) %>%
46 colorbar(title="<b>Liquid \nPenetration [m]</b>")
47
48 CTCP

```

B.2 ANOVA Script

```

1 library(MaxPro)
2 library(SixSigma)
3
4
5 #Factorial Vapor penetration
6 injection.data1 <- ...
  read.csv("/home/olle/OpenFOAM/olle-8/run/Finished.sim.2k.factorial/DoE.factorial/Full.fac.vap.870.csv", ...
  header = TRUE)
7
8 response <- injection.data1$Vapor.penetration
9
10 analyse1 <- aov(response~Injector.D+Injection.U+Chamber.P+Chamber.T +
11 Injector.D * Injection.U + Injector.D * Chamber.P + Injector.D * ...
  Chamber.T +
12 Injection.U * Chamber.P + Injection.U * Chamber.T + Chamber.P*Chamber.T + ...
  Injector.D*Injection.U*Chamber.P +
13 Injection.U*Chamber.P*Chamber.T + Injector.D*Chamber.P*Chamber.T + ...
  Injector.D*Injection.U*Chamber.T
14 , data = injection.data1) ...
  ##Injector.Diameter*Injection.Magnitude*Chamber.Pressure*Chamber.Temperature
15
16 summary(analyse1)
17
18 #Factorial Liquid penetration
19 injection.data2 <- ...
  read.csv("/home/olle/OpenFOAM/olle-8/run/Finished.sim.2k.factorial/DoE.factorial/Full.fac.Liq.pen.870.csv", ...
  header = TRUE)
20
21 response2 <- injection.data2$X
22
23 analyse2 <- aov(response2~Injector.D+Injection.U+Chamber.P+Chamber.T +
24 Injector.D * Injection.U + Injector.D * Chamber.P + Injector.D * ...
  Chamber.T +
25 Injection.U * Chamber.P + Injection.U * Chamber.T + Chamber.P*Chamber.T ...
  + Injector.D*Injection.U*Chamber.P +
26 Injection.U*Chamber.P*Chamber.T + Injector.D*Chamber.P*Chamber.T + ...
  Injector.D*Injection.U*Chamber.T
27 , data = injection.data2)
28
29 summary(analyse2)
30
31 injection.data3 <- ...
  read.csv("/home/olle/OpenFOAM/olle-8/run/FinishedSim.lattice.hyper/DoE.sim/Lattice.hyper.vapor.pen.870.csv", ...

```

```

        header = TRUE)
32
33 response3 <- injection.data3$Vapor.Pen
34
35 analyse3 <- aov(response3~Injector.D+Injection.U+Chamber.P+Chamber.T +
36             Injector.D * Injection.U + Injector.D * Chamber.P + Injector.D * ...
37             Chamber.T +
38             Injection.U * Chamber.P + Injection.U * Chamber.T + Chamber.P*Chamber.T ...
39             + Injector.D*Injection.U*Chamber.P +
40             Injection.U*Chamber.P*Chamber.T + Injector.D*Chamber.P*Chamber.T + ...
41             Injector.D*Injection.U*Chamber.T
42             , data = injection.data3)
43
44 summary(analyse3)
45
46 injection.data4 <- ...
47   read.csv("/home/olle/OpenFOAM/olle-8/run/FinishedSim_lattice_hyper/DoE_sim/Lattice_hyper_liq_pen_870.csv",
48   header = TRUE)
49
50 response4 <- injection.data4$Liquid.Penetration
51
52 analyse4 <- ...
53   aov(response4~Injector.Diameter+Injection.Magnitude+Chamber.Pressure+Chamber.Temperature ...
54   +
55   Injector.Diameter * Injection.Magnitude + Injector.Diameter * ...
56   Chamber.Pressure + Injector.Diameter * Chamber.Temperature +
57   Injection.Magnitude * Chamber.Pressure + Injection.Magnitude * ...
58   Chamber.Temperature + Chamber.Pressure*Chamber.Temperature +
59   Injector.Diameter*Injection.Magnitude*Chamber.Pressure +
60   Injection.Magnitude*Chamber.Pressure*Chamber.Temperature + ...
61   Injector.Diameter*Chamber.Pressure*Chamber.Temperature +
62   Injector.Diameter*Injection.Magnitude*Chamber.Temperature, data = ...
63   injection.data4)
64
65 summary(analyse4)

```

B.3 Latin Hypercube Design

```

1   Lattice_design <- MaxProLHD(16,4)
2
3   Lattice_design$Design[c(1:16)] <- Lattice_design$Design[c(1:16)]*0.0002+0.000096875 ...
4   #Injector diameter
5
6   Lattice_design$Design[c(1:16),2] <- Lattice_design$Design[c(1:16),2]*200+96.875 #injector ...
7   Magnitude
8
9   Lattice_design$Design[c(1:16),3] <- ...
10  Lattice_design$Design[c(1:16),3]*(5056666.667)-54895.833 #Chamber Pressure
11
12  Lattice_design$Design[c(1:16),4] <- Lattice_design$Design[c(1:16),4]*(397.733)+292.82 ...
13  #Chamber Temperature
14
15  data.frame(Lattice_design$Design)
16
17  write.csv(Lattice_design$Design, "~/Desktop/DoE_csvs/Lattice_hyper.csv", row.names = FALSE)

```

B.4 2⁴ Factorial Design And Analysis

```

1   library(SixSigma)
2   library(ggplot2)

```

```

3 theme.update(plot.title = element.text(hjust = 0.5))
4
5 #Reading in data and responses
6 injection.data <- ...
  read.csv("/home/olle/OpenFOAM/olle-8/run/Finished_sim_2k_factorial/DoE_factorial/Full_fac.Liq_pen_870.csv",
  header = TRUE)
7
8 #Designing the 2^4 experiment
9 Experiment.design <- expand.grid(Injector.Diameter = gl(2,1,labels = c('(-)', '(+)')), ...
  Injection.Magnitude = gl(2,1,labels = c('(-)', '(+)')), Chamber.Pressure = ...
  gl(2,1,labels = c('(-)', '(+)')), Chamber.Temperature = gl(2,1,labels = c('(-)', '(+)')) )
10
11 #Randomizing the experiment
12 Experiment.design$ord <- sample(1:16,16)
13 Experiment.design[order(Experiment.design$ord), ]
14
15 #Creating replicates
16 ss.data.doel <- data.frame(repl = rep(1:2, each = 16), rbind(Experiment.design))
17
18 replicate.response <- c(injection.data$X,injection.data$X)
19
20 #Addning response to my data
21 ss.data.doel$response <- replicate.response
22
23 #Aggregating my replicates
24 aggregate(response ~ Injector.Diameter + Injection.Magnitude + Chamber.Pressure + ...
  Chamber.Temperature, FUN = mean, data = ss.data.doel)
25
26 #lm function (Used for conducting analysis of variance)
27 doe.model <- ...
  lm(response~Injector.Diameter+Injection.Magnitude+Chamber.Pressure+Chamber.Temperature +
28     Injector.Diameter * Injection.Magnitude + Injector.Diameter * ...
  Chamber.Pressure + Injector.Diameter * Chamber.Temperature +
29     Injection.Magnitude * Chamber.Pressure + Injection.Magnitude * ...
  Chamber.Temperature + Chamber.Pressure*Chamber.Temperature +
30     Injector.Diameter*Injection.Magnitude*Chamber.Pressure*Chamber.Temperature, ...
  data = ss.data.doel)
31
32 #Summary of the DoE model
33 summary(doe.model)
34
35 #Coefficients for the model
36 coef(doe.model)
37
38 #Estimations for all experimental conditions
39 predict(doe.model)
40
41 #Confidence interval for each factor
42 confint(doe.model)
43
44 #Boxplot for the response
45 boxplot(injection.data$X, main = "Distribution Liquid penetration at 870 μs", ylab = ...
  "Liquid penetration [m]")
46
47
48 #plot the factors and its effect in one plot
49 prinEF <- data.frame(Factor = rep(c("Injector Diameter","Injection Magnitude","Chamber ...
  Pressure", "Chamber Temperature"),each = 2),
50     Level = rep(c(-1,1), 2),
51     Response = c(aggregate(response ~ Injector.Diameter, FUN = mean, data ...
  = ss.data.doel)[,2],
52     aggregate(response ~ Injection.Magnitude, FUN = mean, ...
  data = ss.data.doel)[,2],
53     aggregate(response ~ Chamber.Pressure, FUN = mean, data ...
  = ss.data.doel)[,2],
54     aggregate(response ~ Chamber.Temperature, FUN = mean, ...
  data = ss.data.doel)[,2]))
55 library(ggplot2)

```



```

56 main.effects <- ggplot(prinEF,
57                       aes(x = Level, y = Response)) +
58   geom_point() +
59   geom_line() +
60   scale_x_continuous(breaks = c(-1, 1)) +
61   facet_grid(. ~ Factor) +
62   labs(y="Liquid penetration [m]",title="Effect of factors, Liquid penetration at 870 μs")
63 main.effects
64
65
66
67 #plotting the interactions
68 interactionsCPIM <- aggregate(response ~ Chamber.Pressure + Injection.Magnitude,
69                             FUN = mean, data = ss.data.doe1)
70 effects_interaction <- ggplot(interactionsCPIM, aes(x = Chamber.Pressure, y = response, ...
71           color = Injection.Magnitude)) +
72   geom_point() +
73   geom_line(aes(group = Injection.Magnitude)) +
74   theme(legend.text = element_text(size=15),legend.title = ...
75         element_text(size=12),legend.key.size = unit(1, 'cm'))+
76   theme(title = element_text(face = "bold", color = "black") , axis.text.x = ...
77         element_text(face="bold", color ="black", size=12), axis.text.y = ...
78         element_text(face="bold", color ="black", size=12))+
79   labs(x="Chamber Pressure", y="Liquid penetration [m]",colour="Injection Magnitude", ...
80        title = "Interaction Chamber Pressure and Injection Magnitude")
81 effects_interaction
82
83
84 interactionsIDIM <- aggregate(response ~ Injector.Diameter + Injection.Magnitude,
85                             FUN = mean, data = ss.data.doe1)
86 effects_interaction2 <- ggplot(interactionsIDIM, aes(x = Injector.Diameter, y = response, ...
87           color = Injection.Magnitude)) +
88   geom_point() +
89   geom_line(aes(group = Injection.Magnitude)) +
90   theme(legend.text = element_text(size=15),legend.title = ...
91         element_text(size=12),legend.key.size = unit(1, 'cm'))+
92   theme(title = element_text(face = "bold", color = "black") , axis.text.x = ...
93         element_text(face="bold", color ="black", size=12), axis.text.y = ...
94         element_text(face="bold", color ="black", size=12))+
95   labs(x="Injector Diameter", y="Liquid penetration [m]",colour="Injection Magnitude", ...
96        title = "Interaction Injector Diameter and Injection Magnitude")
97 effects_interaction2
98
99
100 interactionsIDCT <- aggregate(response ~ Injector.Diameter + Chamber.Temperature,
101                              FUN = mean, data = ss.data.doe1)
102 effects_interaction3 <- ggplot(interactionsIDCT, aes(x = Injector.Diameter, y = response, ...
103           color = Chamber.Temperature)) +
104   geom_point() +
105   geom_line(aes(group = Chamber.Temperature)) +
106   theme(legend.text = element_text(size=15),legend.title = ...
107         element_text(size=12),legend.key.size = unit(1, 'cm'))+
108   theme(title = element_text(face = "bold", color = "black") , axis.text.x = ...
109         element_text(face="bold", color ="black", size=12), axis.text.y = ...
110         element_text(face="bold", color ="black", size=12))+
111   labs(x="Injector Diameter", y="Liquid penetration [m]",colour="Chamber Temperature", ...
112        title = "Interaction Injector Diameter and Chamber Temperature")
113 effects_interaction3
114
115
116 interactionsIDCP <- aggregate(response ~ Injector.Diameter + Chamber.Pressure,
117                              FUN = mean, data = ss.data.doe1)
118 effects_interaction4 <- ggplot(interactionsIDCP, aes(x = Injector.Diameter, y = response, ...
119           color = Chamber.Pressure)) +
120   geom_point() +
121   geom_line(aes(group = Chamber.Pressure)) +

```

```

108   theme(legend.text = element.text(size=15),legend.title = ...
      element.text(size=12),legend.key.size = unit(1, 'cm'))+
109   theme(title = element.text(face = "bold", color = "black") , axis.text.x = ...
      element.text(face="bold", color ="black", size=12), axis.text.y = ...
      element.text(face="bold", color ="black", size=12))+
110   labs(x="Injector Diameter", y="Liquid penetration [m]",colour="Chamber Pressure", title ...
      = "Interaction Injector Diameter and Chamber Pressure")
111 effects_interaction4
112
113
114 interactionsCPCT <- aggregate(response ~ Chamber.Pressure + Chamber.Temperature,
115                               FUN = mean, data = ss.data.doe1)
116 effects_interaction5 <- ggplot(interactionsCPCT, aes(x = Chamber.Pressure, y = response, ...
      color = Chamber.Temperature)) +
117   geom_point() +
118   geom_line(aes(group = Chamber.Temperature)) +
119   theme(legend.text = element.text(size=15),legend.title = ...
      element.text(size=12),legend.key.size = unit(1, 'cm'))+
120   theme(title = element.text(face = "bold", color = "black") , axis.text.x = ...
      element.text(face="bold", color ="black", size=12), axis.text.y = ...
      element.text(face="bold", color ="black", size=12))+
121   labs(x="Chamber Pressure", y="Liquid penetration [m]",colour="Chamber Temperature", ...
      title = "Interaction Chamber Pressure and Chamber Temperature")
122 effects_interaction5
123
124 interactionsIMCT <- aggregate(response ~ Injection.Magnitude + Chamber.Temperature,
125                               FUN = mean, data = ss.data.doe1)
126 effects_interaction6 <- ggplot(interactionsIMCT, aes(x = Injection.Magnitude, y = ...
      response, color = Chamber.Temperature)) +
127   geom_point() +
128   geom_line(aes(group = Chamber.Temperature)) +
129   labs(x="Injection Magnitude", y="Liquid penetration [m]",colour="Chamber Temperature", ...
      title = "Interaction Injection Magnitude and Chamber Temperature") +
130   theme(legend.text = element.text(size=15),legend.title = ...
      element.text(size=12),legend.key.size = unit(1, 'cm'))+
131   theme(title = element.text(face = "bold", color = "black") , axis.text.x = ...
      element.text(face="bold", color ="black", size=12), axis.text.y = ...
      element.text(face="bold", color ="black", size=12))
132 effects_interaction6
133
134
135 #Plotting residuals
136 par(mfrow=c(2,2))
137 plot(doe.model)
138 box("outer")
139
140 # Check normality of the residuals
141 shapiro.test(residuals(doe.model))

```